Netherlands Journal of Geosciences

www.cambridge.org/njg

Holocene relative sea-level data for the East Frisian barrier coast, NW Germany, southern North Sea

Friederike Bungenstock[1], Holger Freund[2] and Alexander Bartholomä[3]

[1]Lower Saxony Institute for Historical Coastal Research (NIhK), Wilhelmshaven, Germany; [2]Institute for Chemistry and Biology of the Marine environment (ICBM), Wilhelmshaven, Germany and [3]Department of Marine Research, Senckenberg Institute Wilhelmshaven, Germany

Review

Cite this article: Bungenstock F, Freund H, and Bartholomä A. Holocene relative sea-level data for the East Frisian barrier coast, NW Germany, southern North Sea. *Netherlands Journal of Geosciences*, Volume 100, e16. https://doi.org/10.1017/njg.2021.11

Received: 13 October 2020
Revised: 6 August 2021
Accepted: 20 August 2021

Keywords:
Langeoog; sea-level index points; compaction; basal peats; intercalated peats

Author for correspondence:
Friederike Bungenstock,
Email: bungenstock@nihk.de

Abstract

Collecting sea-level data from restricted coastal areas is essential for understanding local effects on relative sea level. Here, a revised relative mean sea-level curve for the area of the East Frisian island Langeoog, northwestern Germany, for the time period from 7200 cal BP until Recent is presented. The revision is based on the reinterpretation of previously published and unpublished data following the HOLSEA standardisation of data handling. Altogether 68 sea-level data taken from 32 cores and outcrops from Langeoog, its back-barrier and the adjacent mainland, which have been collected since the 1950s for mapping and landscape reconstruction purposes, are presented. The age constraints, derived from radiocarbon ages of basal peat, intercalated peat and molluscs and optical dating of tidal deposits, were evaluated in terms of the HOLSEA sea-level protocol and their stratigraphic context. For 7200 cal BP until modern times, 30 sea-level index points with different uncertainty ranges were defined. Additionally, a factor of decompaction was estimated for the remaining basal peat samples as well as for the underlying sediments of intercalated peat samples.

The comparison of the Langeoog relative sea-level curve with the relative sea-level curve from the western Netherlands shows that the Langeoog curve lies up to 0.80 m lower than the Dutch curve and diverges for the time before 6000 cal BP. Though the offset coincides with the overall predicted trend of glacial-isostatic adjustment, it is less than predicted.

Our study provides a useful assessment of legacy data and contributes to an improved sea-level index dataset for the southern North Sea coast.

Introduction

The response of the coastal zone to global sea-level rise is highly variable. Knowledge of parameters controlling coastal change alongside the regional sea-level history is therefore indispensable when the response to global sea-level rise is to be assessed. The relative sea level (RSL) at any given coastal site depends on different factors such as climatically induced global changes, regional vertical movements of the lithosphere including tectonics and glacial isostatic adjustment (GIA). In addition, local factors influence RSL. These are most notably compaction and coastal geomorphology influencing tides, local water levels and sedimentary processes (e.g. Baeteman, 1999; Kiden et al., 2002; Long et al., 2006; Steffen, 2006; Vink et al., 2007; Kiden et al., 2008; Bungenstock & Weerts, 2012; Karle et al., 2021). These factors act on different time and spatial scales and result in geomorphological changes like progradation and retrogradation of the coastline. Natural hazards such as storm surges may cause severe and abrupt changes to the coastal geomorphology and may trigger long-lasting inundation.

This study presents a reconstruction of RSL for the area of the East Frisian island Langeoog, representative for the East Frisian barrier island coast. A precursor curve was published in Bungenstock & Schäfer (2009). The data points of that curve were derived from intercalated peat data. This was based on the idea that sea-level fluctuations could only be proved by intercalated peat data. However, based on the plotted age data, no sea-level fluctuations in the sense of sea-level drops could be shown. Nevertheless, relying on the idea that intercalated peats clearly indicate a change of RSL, the data points were connected in a step-like manner to hypothesise still-stand phases of RSL instead of sea-level drops as proposed by Behre (2003, 2007). In the following years, there was continuing discussion on the robustness of derived sea-level fluctuations and the resolution of field data to prove these (Bungenstock & Weerts, 2010, 2012; Baeteman, 2011, 2012; Behre, 2012a,b). The standardised 'protocol for a geological sea-level database' (Hijma et al., 2015) and the standardised global synthesis of regional RSL data (Khan et al., 2019) now allow for a reinterpretation of the data of Bungenstock & Schäfer (2009). Therefore, we present a review and reinterpretation of the sea-level data for the area of Langeoog including all available archive data and newly collected data.

CAMBRIDGE UNIVERSITY PRESS

Short review of ideas, opinions and approaches regarding Holocene sea-level research along the German North Sea coast

Research and concepts on Holocene relative sea-level rise along the German North Sea coast have an almost 100-year-long history. The first Holocene RSL curve was published by Schütte (1939). He suggested a sinking coast and no eustasy-related sea-level rise. Relating to the peat layers intercalated in the Holocene sedimentary record along the southern North Sea coast, Schütte assumed an isostatic sinking of the coast interrupted by three rising phases. Nilsson (1949) followed this idea, including the geographical differences of the mean tidal high-water level, to relate data from different areas along the German North Sea coast to each other (see also Louwe Kooijmans, 1976).

Haarnagel (1950) suggested that beside isostasy, eustasy is a relevant factor for RSL along the German North Sea coast. He used basal peat data to exclude errors caused by compaction, and included settlement dynamics to differentiate better amongst transgression and regression phases during the late Holocene (Haarnagel, 1950).

In a seminal paper, Jelgersma (1979) published the RSL curve for the southern North Sea region. She suggested that the controlling factors are eustasy, isostasy and tectonics, with isostasy and tectonics maybe neglibible in the southern North Sea. Her RSL curve is based on radiocarbon data of the base of basal fen peats to avoid errors caused by compaction. The onset of basal fen peat growth can be initiated by local topography and drainage water from the hinterland, which means that fen peat growth is not always in direct correlation with sea level. However, it is not possible to document sea-level fluctuations when data points are exclusively derived from basal peat data (Jelgersma, 1979). In fact, Louwe Kooijmans & Knip (1974) and Roeleveld (1974) interpreted the intercalated peats as indicators for possible sea-level drops.

Kiden et al., (2002) compared the sea-level curves of Jelgersma (1979), Van de Plassche & Roep (1989), Roep & Beets (1988) and Denys & Baeteman (1995) and discussed the influence of spatially variable glacio-hydro-isostatic subsidence along the Belgian and Netherlands coast. They concluded that the local variability is too large to establish a general RSL curve for the southern North Sea region, but that every area of *c.*50 km diameter has its own RSL curve (Kiden et al., 2002). Behre (2003, 2007) published a RSL curve for the entire German North Sea coast. For the last 2000 years he used archaeological data by referring these to mean high water. The problem of different mean high-water levels is solved by referring and correcting all data to the Wilhelmshaven tide gauge (Behre, 2003, 2007). Similar to Jelgersma (1979), Behre regards the glacial isostatic adjustment along the southern North Sea coast as insignificant. His curve is characterised by several wiggles marking sea-level fluctuations of up to 2 m within 200 years.

Ervynck et al., (1999) and Baeteman (1999) related the shifting coastline during the middle and late Holocene to different rates of aggradation when sediment supply outpaces the creation of accommodation space, which could differ from place to place. Baeteman (1999) showed that, for example, a facies shift from mud flat to peat depends on the relative proximity to tidal channels, their migration and sediment supply. Therefore, the intercalated peats are regarded as local phenomena with little significance for RSL reconstruction. With four transects along the East Frisian Peninsula, Streif (2004) showed that the intercalated peat beds have different ages in the different areas apart from the uppermost peat layer situated at −1 to 0 m NN (German Ordnance Datum) which is dated to *c.*2000 BP in all transects.

In addition, intercalated peat beds are always affected by compaction (e.g. Streif 1971; Baeteman, 1999; Bungenstock & Schäfer, 2009; Horton & Shennan, 2009; Engelhart & Horton, 2012) and have to be carefully evaluated before being used for sea-level reconstructions. On the other hand, possible Holocene RSL fluctuations can only be documented by including sea-level index points (SLIPs) from intercalated peat layers sandwiched in the Holocene geological record or by data derived from, for example, foraminifera transfer functions. Plotting data exclusively from basal peat beds could only show possible slowdowns of RSL, but not a sea-level fall (Jelgersma, 1979; Shennan et al., 2005; Brain, 2015). Therefore, in an earlier study (Bungenstock & Schäfer, 2009), data derived from intercalated peat were scrutinised for compaction by interpreting the geological record in cross sections. Additionally, intercalated peat beds were evaluated for their local occurrence versus their stratigraphic meaning by correlating them over several hundreds of metres in cross sections and seismic tracks. This resulted in a RSL curve characterised by phases of slowdown or still-stand. This was in contrast to the strongly fluctuating curve of Behre (2007) and triggered a discussion on the interpretation of sea-level index data in terms of sea-level fluctuations for the German coast (Bungenstock & Weerts, 2010, 2012; Baeteman, 2011; Baeteman et al., 2012; Behre, 2012a,b). Today, most recent sea-level reconstructions for the southern North Sea are based on base of basal peat data or ideally on dated transgressive contacts on top of a thin basal peat layer (Meijles et al., 2018; Hijma & Cohen, 2019). However, the most precise sea-level records, which can be derived from salt-marsh sediments for e.g. the coast of North America (Kemp et al., 2013), Tasmania (Gehrels et al., 2012) or the British Isles (Barlow et al., 2013) and micro-atolls, show maximum oscillations in the order of 0.2 m per century (Gehrels & Shennan, 2015).

Glacial istostatic adjustment (GIA)

Kiden et al. (2002) describe a northwest- to east-southeast-orientated glacial forebulge underneath the coast of the eastern Netherlands and the western German North Sea coast referring to the geophysical isostatic models of Fjeldskaar (1994), Lambeck (1995) and Lambeck et al. (1998). The collapse of this glacial forebulge triggers different glacial isostatic adjustment rates along the southern North Sea coast. Kiden et al. (2002) therefore suggest restricting the collection of sea-level data for a RSL curve to coastal areas smaller than 50 km in diameter. Taking up the approach by Kiden et al. (2002), Vink et al. (2007) compared the RSL curves – all related to mean sea level (MSL) – from Belgium (Denys & Baeteman, 1995), the Netherlands (Jelgersma, 1961; Van de Plassche, 1982; Kiden, 1995; Makaske et al., 2003; Van de Plassche et al., 2005) and the German North Sea coast (Behre, 2003, 2007). They showed that the MSL error band of northwest Germany lies significantly below those of the Netherlands and even more of Belgium, diverging progressively back in time (Vink et al., 2007). The authors therefore concluded that the German North Sea coast has been subject to considerable isostatic subsidence during the Holocene.

Moreover, the glacio-hydro-isostatic model of Steffen (2006) as presented by Busschers et al. (2007, their fig. 10B) shows that the German North Sea coast is situated on the flank of the glacial forebulge and affected by different total uplift depending on the location along the coast. The total uplift differs by more than 20 m from

https://doi.org/10.1017/njg.2021.11 Published online by Cambridge University Press

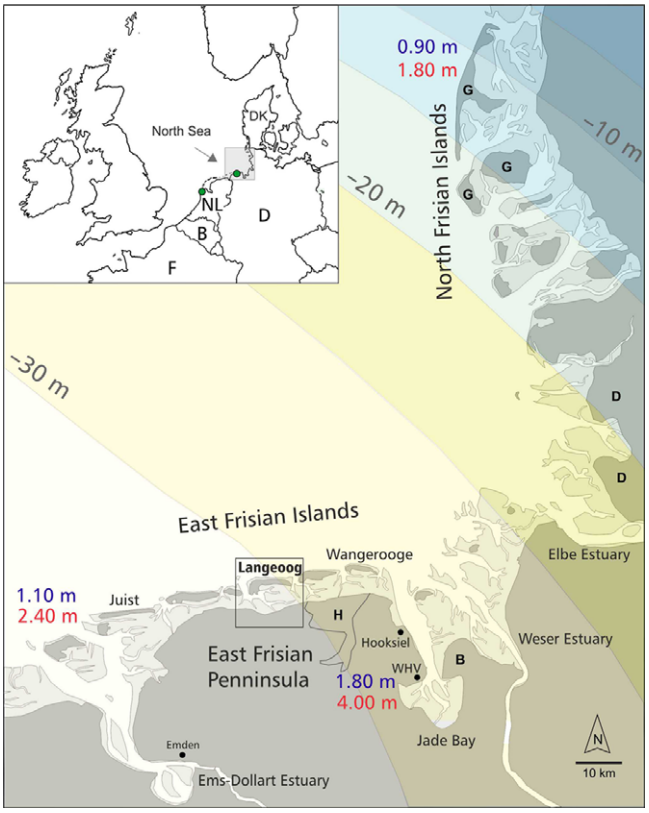

Fig. 1. The German North Sea coast. The modelled glacial isostatic adjustment (GIA) since 21 ka is pictured in shaded zones (according to Steffen, 2006 as presented by Busschers et al., 2007). The different tidal range values along the coast are depicted in red, the mean high-water values in blue. The green dots in the overview frame mark the western Netherlands and study area of Hijma & Cohen (2019) and the East Frisian barrier island coast with the study area of this contribution (see Fig. 8).
G = islands with an outcropping Pleistocene core (Geestinseln); D = Dithmarschen; B = Butjadingen; H = Harle Bay around AD 1400; WHV = Wilhelmshaven.

the western part of East Frisia to North Frisia/Germany since 21 ka (Fig. 1).

Tides

Palaeotidal models of changing tidal range during the Holocene RSL rise in the southern North Sea show an increase in tidal range because of changing bathymetry during inundation of the shelf (Shennan et al., 2000; Van der Molen & de Swart, 2001). While the major changes occurred prior to 6 ka, only minor (cm-scale) to no changes occurred during the subsequent millennia (Shennan et al., 2000; van der Molen & de Swart, 2001). These observations are applied for the open Dutch coast, but there have not been robust observations so far to test, whether the models are valid for the back-barrier areas as well or whether the tidal amplitude may has changed on a larger scale in the tidal basins.

Another aspect to be mentioned is the spatial change of tidal range along the North Sea coast. Today, tidal range varies from lower mesotidal conditions in the west of the German North Sea coast (2.4 m at Borkum, the westernmost island of the East Frisian Peninsula) to upper mesotidal conditions in the centre (Jade Bay with 3.9 m) to lower mesotidal, almost microtidal, conditions in the North (Sylt 1.6 m) (BSH, 2020). Mean high-water level (MHW), being a function of the tidal range, differs by up to 1 m (0.9 m at Sylt and 1.9 m in the Jade Bay) (Fig. 1). Thus, spatially variable tidal ranges have to be assumed for the last millennials depending on the location of the amphidromic points, the bathymetry and the coastal profile. Consequently, the collection of RSL data needs to be restricted to small coastal areas with similar tidal conditions (Bungenstock & Weerts, 2012).

Palaeogeography

Some examples from the German North Sea coast show that changes from semi-closed to open coasts and from a retrograding to a prograding coast and vice versa are not synchronous along the coastline. Instead, these changes strongly depend on local basin configurations and available sediment volumes as also known from the coast in the Netherlands (Beets & van der Spek, 2000; Kiden et al., 2008).

For North Frisia for 7 ka, a peat bed is documented covering a wide coastal area (e.g. Meier et al., 2013). In the northern part of North Frisia, as a result of RSL rise since ~5 ka, Pleistocene plateaus were isolated as so-called *Geest* islands. In the southern part of North Frisia (Dithmarschen) the coast was not protected by Pleistocene plateaus. Since 2 ka the northern part of North Frisia is characterised by continuous erosion during ongoing Holocene RSL rise, while for the southern part a positive sediment budget and, consequently, a prograding coastline is documented (Meier et al., 2013).

For the East Frisian coastline, Flemming & Davis (1994) describe a back-barrier coast existing since 7.5 ka with spit bars accumulating at the Pleistocene ridges of the former landscape, building a closing coast. The system probably changed from micro- to mesotidal conditions around 6 ka (Shennan et al., 2000; Van der Molen & Swart, 2001; Bungenstock, 2005), with an almost closed barrier chain changing to a typical open mesotidal barrier island system and contemporaneously shifting southeastwards during Holocene RSL rise.

On the mainland, Butjadingen (Fig. 1), the land spit between Jade and Weser, prograded ~6 km seaward during the first centuries after AD (Schmid, 1993; Behre, 2012c). Some centuries later, the Harle Bay of ~160 km^2 (Fig. 1) developed at the eastern part of the East Frisian Peninsula (Behre, 1999), later successively reclaimed by embankment.

All these findings underline the importance of collecting sea-level data from relatively small coastal sections, ideally from single tidal basins, to minimise the sources of uncertainties caused by different GIA, tidal conditions and palaeogeographic preconditions on sedimentological processes (Bungenstock & Weerts, 2010, 2012; Baetman et al., 2011). Comparing RSL curves from adjacent tidal basins will help to better understand and even quantify the effects in the respective areas. Therefore, Bungenstock & Weerts (2010) suggest collecting data for RSL curves for the German North Sea Coast representative for five different coastal sections for a first approximation. From west to east, these are (1) the Ems estuary, (2) the East Frisian Barrier island coast (including the barrier island Langeoog), (3a and 3b) the Jade Bay and the Weser estuary, (4) the Elbe estuary and (5) the North Frisian island coast (Fig. 1).

Geographical and geological setting

The German North Sea coast is situated in the southwest of the 'Forchhammersche Linie' (Streif, 1990), which crosses Denmark in the NW–SE direction and which is the hinge line of the glacio-isostatic rebound caused by the postglacial melting of the Scandinavian ice cap. According to the GIA models of Kiden

https://doi.org/10.1017/njg.2021.11 Published online by Cambridge University Press

et al., (2002), Peltier (2004), Steffen (2006) as presented by Busschers et al. (2007), and Vink et al. (2007), the German North Sea is situated on the flank of the collapsing glacial forebulge (Fig. 1).

The German North Sea coast is characterised by tidal flats in a mainly mesotidal regime. The depositional systems are the East Frisian barrier islands, the estuaries of the Ems, Weser and Elbe rivers, the Jade Bay with its narrow connection to the open North Sea, the North Frisian marshland islands and the North Frisian islands with their Tertiary and Pleistocene basements (Fig. 1) and the respective (mostly) back-barrier tidal flats.

In the Ems–Weser–Elbe region, for the East Frisian Peninsula with its barrier coast, the sedimentary record is characterised by Pleistocene glacial deposits disconformably overlain by Holocene sediments up to 25 m thick. The depth of the Holocene base decreases southwards. On the mainland, up to 20 km to the south of the recent coastline, Pleistocene sediments crop out at the surface. The Holocene sedimentary succession starts with a basal peat overlain by sandy, silty and clayey brackish/lagoonal and marine deposits with three to seven intercalated peat beds (Streif, 2004). This documents distinct differences of sedimentation and sedentation processes over relatively short distances along the coast due to non-synchronous coastline shifting, erosion and redeposition (Karle et al., 2021).

The back-barrier zone of Langeoog island

Langeoog is a barrier island situated in a mesotidal system (tidal range of 2.8 m; BSH, 2020). The Holocene sedimentary record in the back-barrier area of Langeoog and its adjacent mainland shows a basal peat, up to several metres thick in places close to the Pleistocene, which crops out directly south of the dike line, and up to four intercalated peat horizons, three of these occurring basin-wide and bearing stratigraphic meaning for the Langeoog area (Bungenstock & Schäfer, 2009).

The Holocene base ranges from −12 m NN to −4 m NN underneath the tidal flats. In the tidal inlets Accumer Ee, west of Langeoog, and the Otzumer Balje, east of Langeoog, and underneath the western part of Langeoog itself, it lies at −22 m NN in palaeo- or active channel structures (NIBIS® Map Server, 2014b).

The dike line separates the tidal flat landscape from the mainland. Since ~700 BP (13th century AD) it was built towards the sea and made the coastline static and unable to react to RSL or single events, whereas Langeoog continuously prograded landward as a consequence of ongoing RSL rise. Maps by Homeier (1964) show a migration of the island of more than 700 m since AD 1650. Over time, the combination of natural and anthropogenic processes enhanced the reworking of the tidal flat sediments (Van der Spek, 1996) and triggered the so-called Wadden Sea squeeze (Flemming & Nyandwi, 1994), which describes the diminishing tidal flats and especially the loss of mudflats (Reineck & Siefert, 1980; Mai & Bartholomä, 2000).

Database and methodology

Langeoog dataset

The Langeoog dataset is based on

(i) the interpretation of 600 cores mainly in the back-barrier of the East Frisian barrier island Langeoog, but also on the mainland and the island itself (NIBIS® Map Server, 2014a, b), three additional cores on the mainland and three outcrops on the island,
(ii) 68 km of Boomer seismic profiles (Bungenstock & Schäfer, 2009),
(iii) 16 radiocarbon ages of intercalated peats provided by the Lower Saxony Survey of Mining, Energy and Geology, Germany – LBEG,
(iv) 26 radiocarbon ages of basal peats provided by the Lower Saxony Survey of Mining, Energy and Geology, Germany – LBEG and from Mauz & Bungenstock (2007);
(v) seven radiocarbon ages from plant material within clastic layers (iii), (iv) and (v) originating from 13 cores drilled within the tidal flat area of Langeoog
(vi) three radiocarbon ages of molluscs from the back-barrier and 11 radiocarbon dates of articulated bivales and gastropods from three outcrops on the island of Langeoog,
(vii) seven ages by optically stimulated luminescence (OSL), samples collected from three cores from the clay district on the mainland directly south of the Langeoog back-barrier (Mauz & Bungenstock, 2007).

For the position of the data see Figure 2.

(i) Core data

Most of the cores were collected by hand-coring systems with 2.7 cm diameter during a mapping programme in the 1960s by the Lower Saxony Survey of Mining, Energy and Geology, Germany – LBEG (NIBIS® Map Server, 2014a). Others were conducted for engineering and hydrological purposes with diameters of up to 10 cm. Their depth reaches from 1 to 25 m below the surface. About 50% of the cores penetrate the base of the Holocene, thus retrieving late Pleistocene sediments, the so-called *Geest*. Core descriptions follow the geological interpretation key of Preuß et al. (1991). The core material was not preserved. As the cores were collected for different purposes, e.g. engineering or hydrogeology, and were recorded by different operators, the quality of the descriptions varies markedly. Therefore, in many cases the descriptions do not allow a detailed interpretation of the geological record. The additional cores and samples on Langeoog island and on the mainland were collected during the last 20 years.

During the 2000s the starting levels of all archive cores have been corrected by the LBEG on the basis of the DTM5. Griffel et al. (2013) describe extreme differences between many of the corrections and the originally listed starting levels, due to subsequently built harbour sites and dikes. Therefore, we tested our core list for plausibility. According to the DTM5 control, we corrected the starting point for cores GE187 with HV4182, HV4183 and HV4184 by 0.38 m upwards, and for GE189 with HV4180 and HV4181 according to the DTM5 correction by 0.79 m upwards. The original documented starting level of core GE193 – and respectively the sample depths of HV4185, HV4186, HV4187 and 4188 – differs from that corrected by the DTM5 and depicted in the NIBIS® Map Server (2014) by 1.57 m. In the LBEG database, GE193 is registered with −0.10 NN, whereas in the NIBIS® Map Server (2014) it is plotted with 1.43 m. As the core position on the topographic map is almost exactly on the zero-line, for reasons of plausibility the value from the original database was retained.

(ii) Seismics

The reflection seismic survey used a GeoPulse Boomer System (280 J maximum output energy at 3.5 kHz). Maximum penetration was ~.40 m with less than 0.5 m resolution (55 m two-way travel time (TWTT), 8400 Hz to 12 kHz frequency). The seismic surveys have

https://doi.org/10.1017/njg.2021.11 Published online by Cambridge University Press

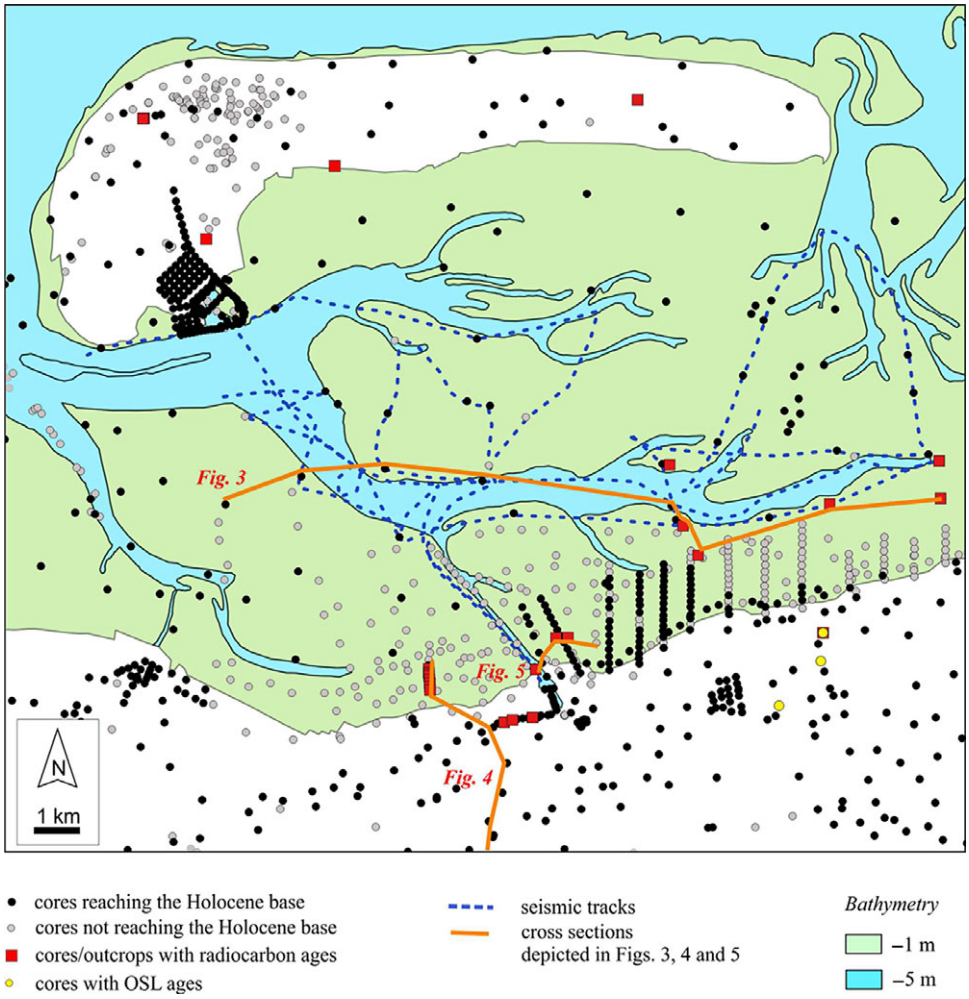

Fig. 2. Langeoog island, its back-barrier tidal flats and the adjacent mainland with the data analysed for this study. The cross sections are chosen to especially depict the age data that have been finally defined as reliable sea-level index points for the time between 7200 and 3000 cal BP, and are depicted in Figures 3, 4 and 5.

been carried out depending on maximum water level. Tidal flats were crossed only during high tide (Fig. 2). Altogether 68 km of seismic survey lines have been collected and were linked with the cores on the basis of the sub-bottom surface bathymetry. For further details and seismic plots, see Bungenstock & Schäfer (2009).

(iii), (iv), (v) and (vi) Radiocarbon data of peats and molluscs

The ^{14}C age determinations (bulk) were performed by the LBEG and the Poznań Radiocarbon Laboratory, Poland (Table 1). The results were calibrated using CALIB (Version 8.2), IntCal20 and Marine20 (Reimer et al., 2020).

All ages from shells were derived from articulated *in situ* specimens. The specimens of the gastropod *Peringia ulvae* were collected from the stratigraphically important layer 'Hydrobien-Schichten' of Langeoog (Barckhausen, 1969). According to measurements of Enters et al. (2021) the delta R value for reservoir correction of ages originating from *in situ* shell material was applied with −85 ± 17.

All radiocarbon data are plotted with the 2σ error (Figs 3, 4, 5 and 6).

(vii) OSL data

The OSL age determination was performed by the OSL laboratory at the Department of Geography of the University of Liverpool, UK. Samples were treated following the preparation procedures for silt-sized quartz grains samples for multiple-grain aliquots (Mauz et al., 2002). Although 'variable bleaching rules' in tidal-flat sub-environments have to be considered, OSL dates from tidally deposited sediments show consistent chronologies (Mauz et al., 2010; Zhang et al., 2014). For a detailed description of the samples used see Bungenstock (2006) and Mauz & Bungenstock (2007).

Indicative meaning of the peat

Age data were taken from basal as well as from intercalated fen peats.

Studies on coastal landscape reconstruction, sea-level and peat data show height differences of up to several metres for peat of the same age. This demonstrates the independence of several basal peat formations from sea level due to local hydrography, which has been described before by Jelgersma (1961), Lange & Menke (1967), Van de Plassche (1982), Wolters et al., (2010), Hepp et al., (2019) and Karle et al., (2021) for the North Sea. As no plant macro-remains or pollen data are provided for the peat samples, which could prove a marine influence, age data of the basal peat beds are tested for their reliability in terms of sea-level data by their position in cross sections (see Figs 3, 4 and 5) and in the age–depth diagram (Fig. 6). Based on this analysis the basal peat beds are classified either as

https://doi.org/10.1017/njg.2021.11 Published online by Cambridge University Press

Table 1. Summary of the indicative meanings of the different sample types in the Langeoog area. The samples providing upper-limiting data are collected from fen-wood peat or carr peat. For those the reference water level is the ground water level (GWL) and additionally specified in the table. In the Langeoog back-barrier area, MHW is at 1.42 m MSL, MTL is at 0.10 m. For more detailed information on tide levels see the Supplementary Material available online at https://doi.org/10.1017/njg.2021.11

Sample type	Evidence	Reference water level	Indicative range
Fen peat / *Carex* peat / Fen and *Carex* peat	Generally consisting of Phragmites or Phragmites–*Carex* peat, the average water depth is set at 0.3 m and indicative range at 0.2 m (Hijma & Cohen, 2019)	MHW − 0.3 m	(MHW − 0.3) ± 0.2 m
Fen-wood peat/ carr peat	This peat generally formed in *Alnus–Salix* swamps (Bos et al., 2012), modern analogues formed very close to average water levels (Clerkx et al., 1994, cited in Hijma & Cohen, 2019)	MHW When selected as upper-limiting data: GWL	MHW ± 0.1 m (after Törnqvist et al., 1998) Indicative range when selected as upper-limiting data: GWL ± 0.1 m
Peat, undifferentiated	Assuming that bog peats can be excluded, for peat beds not further specified we apply 0.2 m as average water depth and ±0.3 m as indicative range to cover the full range of water depths in which fen-wood or fen peat generally forms following Hijma & Cohen (2019)	MHW − 0.2 m	(MHW − 0.2) ± 0.3 m
Humous and peaty sediments	Organic material for radiocarbon dating is taken from intertidal sediments. As these are characterised by plant material and roots and often peaty material, they are interpreted to originate from the upper tidal area	(MHW + MTL)/2	MHW − MTL
Brackish-lagoonal sediments	This facies develops in a subaquatic to semi-terrestrial environment of coastal lagoons and belts of reed. It is often observed in a transition zone between marine silting-up zones and semi-terrestrial fen peat (Karle et al., 2021). We therefore assume the upper part of tidal range	(MHW + MTL)/2	MHW − MTL
Intertidal	Typical intertidal sediments partly clayey to silty, partly sandy and with tidal lamination are described. They generally form between MHW and MLW	MTL	MHW - MLW
Molluscs	As the dated molluscs are all taken from tidal flat sediments they indicate a reference water level between MLW and MHW. As this is already a generalised value, we do not apply an additional indicative range. The bivalves live in burrows with different depth to the surface. We add the respective values to the particular molluscs with a correct citation for the burrow depth indicated separately.	MTL	MHW − MLW
Cerastoderma edule	see above; burrow depth to 0.03 m (Hertweck, 1993)	MTL – 0.03 m	(MHW – MLW) − 0.03 m
Mya arenaria (spec.)	see above; burrow depth to 0.35 m (Hertweck, 1993)	MTL – 0.35 m	(MHW – MLW) − 0.35 m
Scrobicularia plana	see above; burrow depth to 0.15 m (Hertweck, 1993)	MTL – 0.15 m	(MHW – MLW) − 0.15 m
Peringia ulvae	Any position within tidal range, see text (Newell, 1962, Barckhausen, 1969)	MTL	MHW – MLW

sea-level index points or as upper-limiting data points. The top of a basal peat is often a sea-level index point when non-erosively overlain by brackish–marine sediments (Hijma et al., 2015), which is not the case in the available dataset of this study.

Fen peats are nourished by groundwater, which, consequently, influences the peat's growth. Groundwater level, in turn, is often controlled by sea level in coastal areas and it is generally accepted that basal peat within coastal zones starts forming at local MHW level (Van de Plassche, 1982; Hijma & Cohen, 2019). The better the peat is characterised for its plant association, the more precisely its relation to MHW can be defined, as shown by Den Held et al., (1992), Clerkx et al., (1994), Berendsen et al., (2007) and Bos et al., (2012). The different kinds of fen peats of the presented database are listed in Table 1, with their respective relation to MHW as derived from literature.

The same relation applies for intercalated peats. Certainly, for intercalated peats compaction of underlying sediments is a crucial issue to consider. Thus, intercalated peats provide additional information (Engelhart & Horton, 2012), but have to be carefully evaluated for their deposition *in situ*, their stratigraphic meaning (e.g. reworked or not) and compaction of underlying sediments.

Indicative meaning of the mollusc samples

Only articulated shells in living position were dated. These are *Cerastoderma edule* (Linnaeus 1758), *Scrobicularia plana* (da Costa 1778), *Mya arenaria* (Linnaeus 1758) and *Mya truncata* (Linnaeus 1758), all sampled from intertidal sediments from outcrops on Langeoog island. They are plotted with the full tidal range as error envelope (s. Table 1). Furthermore, it is worth considering that the associated burrows reach different depths: *Cerastoderma edule* burrows down to 3 cm (Klausnitzer 2019), *Scrobicularia plana* to 15 cm (Hertweck, 1993) and *Mya arenaria* to 35 cm (Hertweck, 1993). Therefore, they refer to mean tidal level (with the full tidal range as indicative range) minus the respecitve burrow depth (see Table 1).

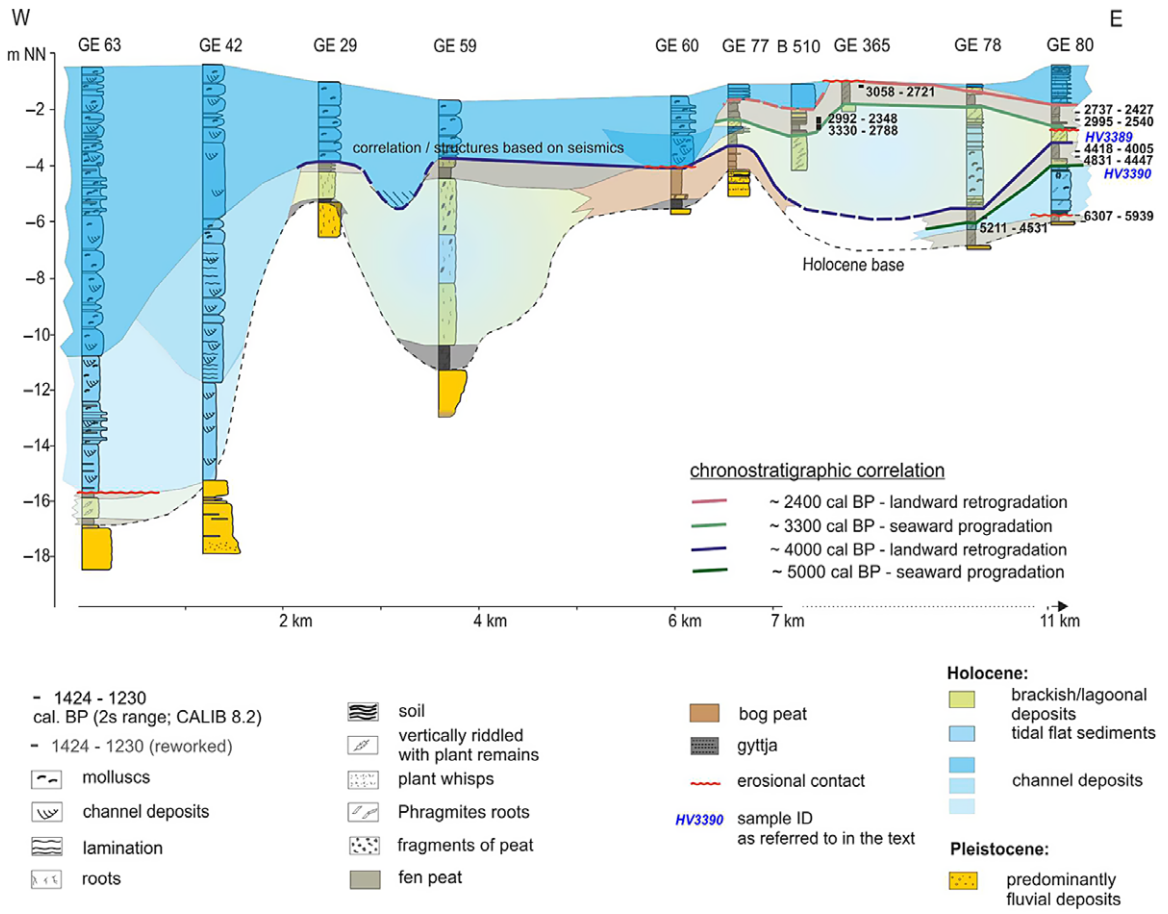

Fig. 3. West–east cross section 'Stüversledge' and chronostratigraphic correlations. For the osition of the cross section see Fig. 2.

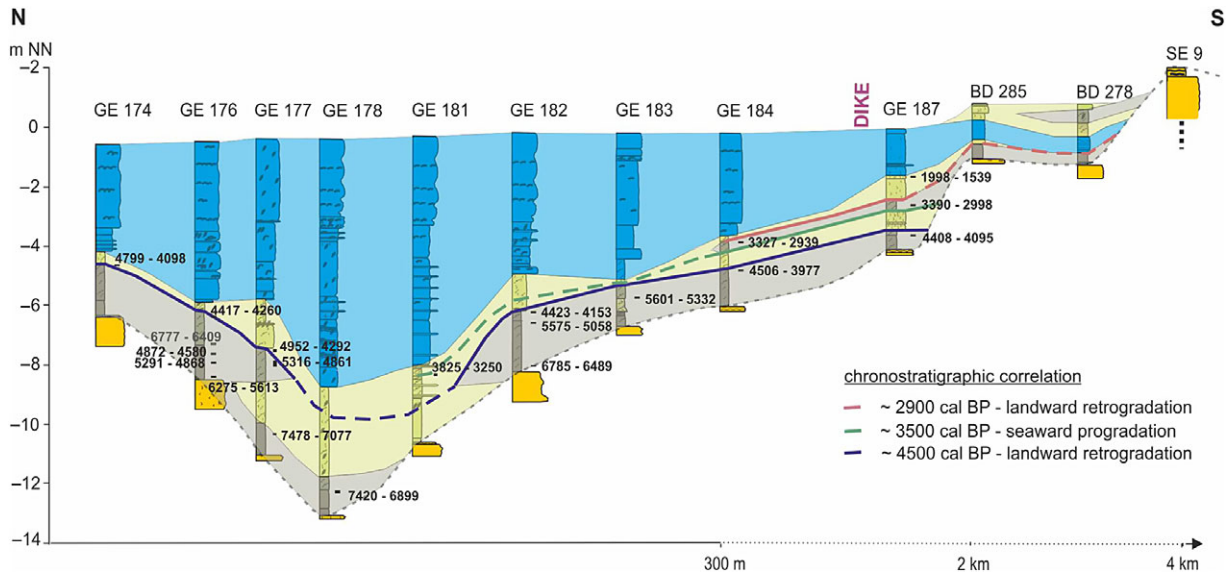

Fig. 4. North–south cross section 'Damsumer Sand' and chronostratigraphic correlation. For the legend, see Fig. 3, for the position, see Figure 2.

Additionally, four radiocarbon datings of the gastropod *Periniga ulvae* (formerly *Hydrobia ulvae*) are available. *Peringia ulvae* reaches its maximum density at approximately mid-tide level, but it also floats during high tide and burrows in the sand during low tide (Newell, 1962). *Peringia ulvae* can reach densities of over 370,000 individuals per square metre (Schückel et al., 2013). At the former southern rim of Langeoog island, a layer of *Peringia ulvae* stretches ~10 km in the N–S direction and over 3 km in the W–E direction. It is described as stratigraphic key layer, the so-called *Hydrobienschicht* (*Hydrobia* layer) marking a former island

https://doi.org/10.1017/njg.2021.11 Published online by Cambridge University Press

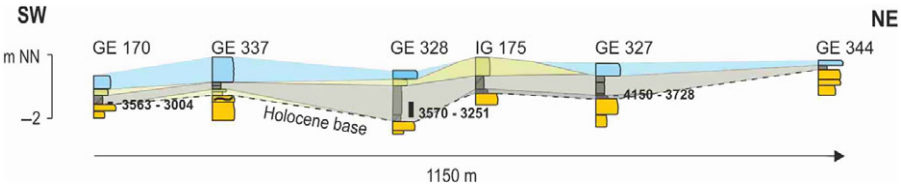

Fig. 5. SW–NE cross section 'Hungatplate'. For the legend, see Figure 3, for the position see Figure 2.

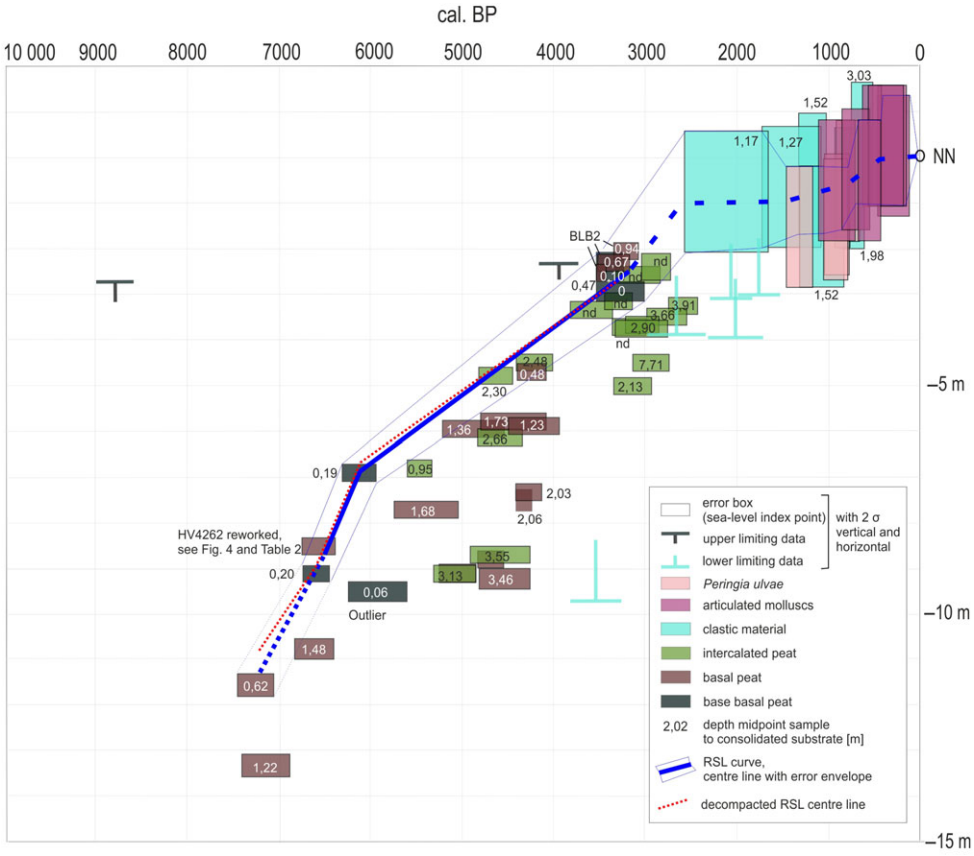

Fig. 6. The complete dataset for the Langeoog area.

position (Barckhausen, 1969). Following Barckhausen (1969) it developed at the southern rim of the former island Langeoog in shallow and quiet water with plenty of algae food supply for *Peringia ulvae*. Maybe it was even protected by surrounding sand bars, which prevented uplift and transport of the snale during high water. However, *Peringia ulvae* accumulated there and obviously did not drift away. The *Perinigia ulvae* ages sampled from the 'Hydrobienschicht' also refer to mean tide level with the full tidal range as indicative range.

Indicative meaning of the samples dated by OSL

The OSL samples are plotted with their original depth plus the full tidal range as error range, as no indicative meaning other than 'deposited within tidal range' can be deduced. This is in contrast to Mauz & Bungenstock (2007) who suggest an indicative meaning based on assumptions of the position of the samples in the upper, middle or lower third of the tidal range based on the macroscopic facies description, but without robust microfauna analyses. The OSL samples are defined as sea-level index points, as MSL cannot lie lower or higher than the full error range of these samples.

Uncertainties

All age data are plotted with the 2σ error. For calculation of the vertical error we follow the HOLSEA workflow. All uncertainties are filled in the 77-field sea-level spreadsheet provided by Khan et al., (2019) (see Supplementary Material available online at https://doi.org/10.1017/njg.2021.11). For more information about the now standardised uncertainties to be regarded, see Hijma et al., (2015) and Khan et al., (2019).

Compaction

Compaction as a term used in the following comprises auto-compaction and compression. Auto-compaction is a non-mechanical diagenetic process including structural collapse, biological decay and chemical alteration of organic matter. Compression mainly depends on the overburden. It concerns all kinds of unconsolidated deposits.

Bennema et al., (1954) describe peat compaction of maximal 85–90%; Kaye & Barghoorn (1964) observe peat compaction of 80–90% for samples from the North American coast. In these cases, a correction factor for decompaction of at least 5 has to be applied.

Denys & Baeteman (1995) assume an average compaction of 50% (correction factor 2). Roeleveld & Gotjé (1993) apply a minimum and maximum correction factor of 0 and 3, which is modified by Van de Plassche et al., (2005) and Berendsen et al., (2007) to a correction factor of 1.5 for the base of the dated sample and a correction factor of 2.5 for the top of the dated sample. Although Van de Plassche et al., (2010) state that Berendsen et al., (2007) used 2.5 and 3.5 as correction factor instead of 1.5 and 2.5 as written in the text, it is not clear which correction factor is the correct one and whether the 2.5 and 3.5 factor had also been used before by Van de Plassche et al., (2005), which was cited by Berendsen et al., (2007). However, Khan et al., (2019) suggest applying a factor of 2.5 for the correction of the sample thickness referring to Van de Plassche et al. (2005), Van Asselen (2011) and Hijma et al., (2015).

Smith et al., (2003) and Lloyd et al., (2013) estimate peat compaction underneath clastic sediments by 40–68%, which is a factor between 1.66 and 3.125. If the thickness of the clastic overburden exceeds 2.5 m, they assume that the compaction of the underlying peat has been completed before the deposition of another regressive layer such as an intercalated peat bed.

For fine-grained sediments which suffered post-depositional compression, the model for decompaction published by Paul & Barras (1998) gives an average depth correction of 5–10% of the layer thickness.

These approaches are useful when the local data densities allow detailed observation of compaction rates; unfortunately, this is often not the case. Any correction would then lead to inaccuracies and eventually even falsify the original data further (Edwards, 2006; Engelhart & Horton, 2012). Thus, the data are classified into base-of-basal, basal and intercalated peat in the age–depth diagram to take the different compaction potential into account for the interpretation of the sea-level data (Shennan et al., 2000; Horton & Shennan, 2009; Engelhart & Horton, 2012). Additionally, after tackling the best data for the drawing of the RSL curve, we measured the distances of the compaction-prone samples to the consolidated Pleistocene basement and to the centre line of our RSL curve as an approach to suggest a factor of decompaction for our study area.

Ideally, the base of basal peat is positioned directly, or only few centimetres, above the Pleistocene basement. For the dataset presented here, no data point applies for these prerequisites. The base-of-basal peat data are therefore defined as such if positioned a maximum of 0.20 m above the Pleistocene, to differentiate them from other basal peat data in our dataset, which are positioned 0.45–3.41 m above the Pleistocene. The samples defined as base of basal peat data vary between 5 and 10 cm thickness. Of course, they also comprise a compaction uncertainty. Nevertheless, they provide the best data of the dataset available for the Langeoog area.

Sea-level index points

The indicative meaning of every data point has been calculated following the principles of the HOLSEA workflow (Khan et al, 2019; see Table 1; Supplementary Material available online at https://doi.org/10.1017/njg.2021.11). Sea-level index points and lower- and upper-limiting data are differentiated and are plotted in an age–depth diagram (Fig. 6). The sea-level index points were evaluated as such following three criteria: (1) the original sample description; (2) the correlation within cross sections (Figs 3, 4 and 5) and seismic profiles to evaluate the data for compaction and whether they can be correlated over several hundred metres to exclude local reworking and transport (see Bungenstock & Schäfer, 2009); and (3) the position in the age–depth diagram (Fig. 6).

Results and interpretation

Progradation and retrogradation: signals in the sedimentary record

In Table 2, all samples with their 2σ age range, sample depth and indicative meaning for RSL are listed, together with the core they are taken from, to give a general overview and to better identify the samples in the cross sections (Figs 3, 4 and 5). For details of facies description and error ranges see the Supplementary Material available online at https://doi.org/10.1017/njg.2021.11.

In the study area intercalated peat beds, which are representative for a local seaward progradation of the coastline, form after the deceleration of RSL ~6000 cal BP. The first one dates to 5600 cal BP, the last one ends at 2500 cal BP (Figs 3 and 4). For a short period from 4000 to 3800 cal BP, no intercalated peat beds are documented in the study area (Fig. 6). The reason for this transgressional phase is not clear. The RSL for Langeoog shows neither an acceleration, nor an increase in energy, which would be suggested by erosional contacts, sand layers or even shell layers but which are not documented in the cores (see Figs 3 and 4). However, after ~2500 cal BP, intertidal marine deposition dominates throughout the study area in parts with an erosional contact on top of the underlying brackish–lagoonal sediments and peats (Figs 3 and 4).

Langeoog RSL curve

The age–depth diagram in Figure 6 shows the entire dataset plotted with its indicative meaning for MSL as reference water level and the vertical and horizontal 2σ error. Additionally, for every sample the depth from the midpoint to the consolidated substrate (Pleistocene) is plotted.

Out of the 68 sea-level data, 30 are used as sea-level index points. Four of those are of relatively strong quality in terms of vertical uncertainty ranges. The oldest sea-level index point is compaction-prone but the best one available for that time, five data points are lower-limiting data, at least two data points (probably five, see discussion about the peat data in BLB2) are upper-limiting data. Most rejected data were rejected due to strong compaction (Table 2; Supplementary Material available online at https://doi.org/10.1017/njg.2021.11). The 2 σ error boxes of the chosen samples are connected to depict the RSL error envelope (Fig. 6). All chosen samples are marked in Table 2 and plotted in Figures 3, 4 and 5.

For ~6700 to 3000 cal BP, four sea-level index points are derived from the base of the peat layer with a depth between 0 and 0.20 m to the consolidated substrate (Pleistocene). The error envelope for ~6700 to 3000 cal BP is depicted by connecting the error boxes of these four sea-level index points. The error envelope is complemented for the period since ~7200 cal BP by the best sea-level index point available, which is a sample taken from a basal peat with 0.62 m depth to the Pleistocene. Further supporting data, which plot within the error envelope, are derived from four basal peat data with 0.45–0.94 m depth to the Pleistocene. Additionally, it should be mentioned that five samples from intercalated peats with 2.30 m, 2.48 m and unknown depth to the Pleistocene also plot in the error envelope. The RSL curve starts with a rise of 0.40 m per century and decelerates to 0.16 m per century since ~6000 cal BP.

For 3000 cal BP to Recent, 18 SLIPs are available, with a wide vertical uncertainty range. For the upper boundary of the error envelope the lowest error boxes, and for the lower boundary of the error envelope the uppermost error boxes, are connected. As there is a wide uncertainty range, a reliable course of RSL is hard

https://doi.org/10.1017/njg.2021.11 Published online by Cambridge University Press

Table 2. List of all available data for the Langeoog area as plotted in Figure 6. The samples analysed are legacy data from different projects and not taken originally for sea-level research. Therefore, many of them are not taken at transgressive contacts, but in the middle or in the upper or lower parts of a peat layer. Lab numbers of the samples evaluated as reliable for the RSL curve are marked in boldface. The oldest sea-level index point, which is used for the curve although it is compaction-prone, is underlined. The 2σ age range is listed in the fourth column. The peat data are calibrated with Calib 8.2, Intcal20 (Reimer et al., 2020), the mollusc data are calibrated with Calib 8.2, Marine 20 (Reimer et al., 2020). Delta R −85 ± 17 (Enters et al., 2021) and the OSL data are corrected to BP. Dat. (third) column specifies the dating method, SLIP stands for sea-level index point, nd stands for not defined, n/a stands for not applicable. Further details about the facies, calculation of errors and the indicative meaning are listed in the Supplementary Material available online at https://doi.org/10.1017/njg.2021.11

Core	Lab.-No.	Dat.	(cal) BP-2σ (Calib 8.2)	Depth (m NN)	Sample type	RSL (m NN)	Classification	Reason for rejection
	HV1632	rc	2846–2395	−1.43	Fen peat	−2.55	SLIP	
	HV1633	rc	3455–3161	−2.03	Fen peat	−3.15	SLIP	
	HV1634	rc	3825–3368	−2.23	Fen peat	−3.35	SLIP	
GE 78	HV3394	rc	5211–4531	−5.85	Basal fen peat	−6.97	SLIP	Compaction
GE 80	HV3387	rc	2737–2427	−2.09	Intercalated fen peat	−3.21	SLIP	Compaction
GE 80	HV3388	rc	2995–2540	−2.35	Intercalated fen peat	−3.47	SLIP	Compaction
GE 80	HV3389	rc	4418–4005	−3.47	Intercalated fen peat	−4.59	SLIP	
GE 80	HV3390	rc	4831–4447	−3.68	Intercalated fen peat	−4.80	SLIP	
GE 80	**HV3391**	rc	6307–5939	−5.78	Base of basal fen peat	−6.90	SLIP	
GE 81	HV3393	rc	4845–4360	−5.06	Intercalated fen peat	−6.18	SLIP	Compaction
2210/GE 84	HV1998	rc	901–503	1.56	Soil	n/a	Upper limiting	Dunal slack, beyond any relation to sea level
GE 84	HV1999	rc	3149–1949	0.37	Intertidal sediment	0.27	rejected	Allochthonous material (reported in LBEG database
GE 170	**HV2652**	rc	3563–3004	−1.55	Wood from basal carr and fen peat	−2.97	SLIP	
GE 170	HV2651	rc	9000–8606	−1.55	Basal carr and fen peat	−2.97	Upper limiting	Totally independent of sea level
GE 174	HV4264	rc	4799–4098	−4.68	Basal fen and *Carex* peat	−5.80	SLIP	Compaction
GE 176	HV4261	rc	4417–4260	−6.44	Basal fen peat	−7.56	SLIP	Compaction
GE 176	HV4262	rc	6777–6409	−7.38	Basal fen peat	−8.50	rejected	Reworked (inconsistent chronology)
GE 176	HV4728	rc	4872–4580	−7.68	Basal *Carex* peat	−8.80	SLIP	Compaction
GE 176	HV4729	rc	5291–4868	−7.98	Basal fen peat	−9.10	SLIP	Compaction
GE 176	HV4263	rc	6275–5613	−8.45	Base of basal fen peat	−9.57	SLIP	Outlier
GE 177	HV4270	rc	4952–4292	−7.61	Intercalated fen peat	−8.73	SLIP	Compaction
GE 177	HV4271	rc	5316–4861	−8.02	Intercalated fen peat	−9.14	SLIP	Compaction
GE 177	HV4272	rc	7478–7077	−10.50	Basal fen peat	−11.62	SLIP	
GE 178	HV4732	rc	7420–6899	−12.27	Basal carr peat	−13.39	SLIP	Compaction
GE 181	HV4265	rc	3825–3250	−8.28	*Phragmites* roots in brackish–lagoonal sediments	−9.04	Lower limiting	Compaction
GE 182	HV4267	rc	4423–4153	−6.23	Basal fen peat	−7.35	SLIP	Compaction
GE 182	HV4268	rc	5575–5058	−6.58	Basal fen peat	−7.70	SLIP	Compaction
GE 182	**HV4269**	rc	6785–6489	−8.03	Basal fen peat	−9.15	SLIP	
GE 183	HV4730	rc	5601–5332	−5.75	Intercalated fen peat	−6.87	SLIP	Compaction
GE 184	HV4731	rc	3327–2939	−3.90	Intercalated fen peat	−5.02	SLIP	Compaction
GE 184	HV4266	rc	4506–3977	−4.83	Basal fen peat	−5.95	SLIP	Compaction
GE 187	HV4182	rc	1998–1539	−1.63	*Phragmites* roots in lagoonal sediments	−2.39	Lower limiting	
GE 187	HV4183	rc	3390–2998	−2.57	Intercalated fen and *Carex* peat	−3.69	SLIP	Compaction

(*Continued*)

Table 2. (*Continued*)

Core	Lab.-No.	Dat.	(cal) BP-2σ (Calib 8.2)	Depth (m NN)	Sample type	RSL (m NN)	Classification	Reason for rejection
GE 187	HV4184	rc	4408–4095	–3.62	Basal fen and *Carex* peat	–4.74	SLIP	
GE 189	HV4180	rc	2302–1846	–1.77	Roots in brackish–lagoonal sediments	–2.53	Lower limiting	Compaction
GE 189	HV4181	rc	3210–2852	–2.56	Intercalated fen peat	–3.68	SLIP	Compaction
GE 193	HV4185	rc	2349–1706	–2.53	*Phragmites* roots in lagoonal sediments	–3.29	Lower limiting	Compaction
GE 193	HV4186	rc	3141–2744	–3.35	Intercalated fen peat	–4.47	SLIP	Compaction
GE 193	HV4187	rc	4830–4297	–8.15	Basal fen and *Carex* peat	–9.27	SLIP	Compaction
GE 193	HV4188	rc	6845–6408	–9.73	Basal fen and *Carex* peat	–10.85	SLIP	Compaction
GE 327	HV1892	rc	4150–3728	–1.03	Wood in transition from gyttja to basal fen peat	–2.45	Upper limIting	
GE 328	**HV1893**	rc	3570–3251	–1.25	Basal fen peat	–2.37	SLIP	
GE 365	HV1894	rc	3058–2721	–1.20	Intercalated peat	–2.42	SLIP	
B510	HV1635	rc	2992–2348	–2.43	Peaty sediments	–3.19	Lower limiting	
B510	HV1636	rc	3330–2788	–2.65	Intercalated fen peat	–3.77	SLIP	Compaction
N.N. 1	HV1630	rc	3510–3780	nd	*Cerastoderma edule* in driftline	n/a	rejected	No depth information
N.N. 2	HV956	rc	622–233	nd	Shell detritus	n/a	rejected	No depth information
BLB 2	**LV02**	OSL	1330–1010	–0.23	Tidal flat sediments	–0.33	SLIP	
BLB 2	**LV03**	OSL	1730–1090	–0.53	Tidal flat sediments	–0.63	SLIP	
BLB 2	**LV04**	OSL	2580–1660	–0.65	Tidal flat sediments	–0.75	SLIP	
BLB 2	KIA21893	AMS	3339–3083	–0.92	Basal fen peat	–2.04	Upper limiting	
BLB 2	KIA21894	AMS	3354–3176	–1.19	Basal fen peat	–2.31	Upper limiting	
BLB 2	KIA21895	AMS	3562–3456	–1.40	Basal fen peat	–2.52	Upper limiting	
BLB 4	**LV06**	OSL	930–770	–0.57	Tidal flat sediments	–0.67	SLIP	
BLB 5	**LV08**	OSL	750–510	0.44	Tidal flat sediments	0.34	SLIP	
BLB 5	**LV09**	OSL	890–610	–0.56	Tidal flat sediments	–0.66	SLIP	
BLB 5	**LV10**	OSL	1310–830	–1.41	Tidal flat sediments	–1.51	SLIP	
LADQ42/2	**Poz-25927**	rc	1474–1179	–1.43	*Peringia ulvae*	–1.53	SLIP	
LADQ42/1	**Poz-25926**	rc	916–659	–0.40	*Peringia ulvae*	–0.50	SLIP	
LADQ4/13	**Poz-25924**	rc	1077–775	–1.16	*Peringia ulvae*	–1.26	SLIP	
LADQ4/14	**Poz-25925**	rc	1091–785	–1.24	*Peringia ulvae*	–1.34	SLIP	
LA71/1	**HV-22944**	rc	441–69	0.00	*Mya arenaria*	0.25	SLIP	
LA72/2	**HV-22947**	rc	484–112	0.00	*Scrobicularia plana*	0.05	SLIP	
LA72/3	**HV 22948**	rc	497–165	0.00	*Mya arenaria*	0.25	SLIP	
LA71/2	**HV 22945**	rc	542–172	0.00	*Mya arenaria*	0.25	SLIP	
LA2/72	**HV 24577**	rc	667–417	–0.20	*Cerastoderma edule*	–0.27	SLIP	
LA2/72	**HV 24576**	rc	841–541	–0.20	*Cerastoderma edule*	–0.27	SLIP	
LA72/1	**HV 22946**	rc	1112–703	–0.75	*Mya spec.*	–0.50	SLIP	

https://doi.org/10.1017/njg.2021.11 Published online by Cambridge University Press

to estimate. Nevertheless, a deceleration of RSL seems to be apparent since ~2500 cal BP.

Estimation of compaction on basal and intercalated peat beds

As the dataset comprises base-of-basal peat data on which the RSL curve is based, the compaction effect of all other data becomes obvious and is, as expected, dependent on the thickness and the material of the deposits underneath the respective sample. In Figure 6 the distance of the midpoint of every sample to the Pleistocene is plotted. The compaction of every sample is estimated by simply measuring the vertical distance from the midpoint of the respective sample to the centre line of the RSL curve. In Tables 3 and 4 the factor necessary to decompact a sample to plot it on the centre line of our RSL curve is calculated. While the average decompaction factor for basal peats is calculated with 2.29, the average decompaction factor for intercalated peats is 1.67. The basal peats HV4728, HV4729 and HV4263 – all taken from core GE176 (Fig. 4) – are excluded as outliers as their decompaction factors far exceed the factors of the other samples. This means, when decompacting the basal peat data with the factor 2.29 and the intercalated peat data with 1.67, all data (except the above-mentioned outliers) plot at least within the error band.

A compaction-corrected RSL curve resulting from applying the calculated decompaction factor of 2.29 on the base of basal peat data is plotted in Figure 6 as red dotted line.

Discussion

Compaction of basal peats and sediments below intercalated peat samples

In Figure 6 the depth to consolidated substrate for the sea-level index points from 7200 to 3000 cal BP is depicted in the data error boxes. In Tables 3 and 4 the compaction rates and the respective factors of decompaction are calculated based on the dataset, that allows for reconstructing the RSL curve, with data lacking between 6000 and 3000 cal BP resulting in a straight line in between the chosen data (Fig. 6). For the RSL curve, especially the samples lying not more than 20 cm above the Pleistocene deposits have been used. Most other samples show a clear impact of compaction with up to 55% (HV4731 from core GE184, Fig. 4)), although there are some exceptions, such as HV3389 and 3390 from core GE80 (see Fig. 3) with only 5% and 16% of compaction (Table 4), or the peat samples from BLB2 lying in the upper part of the RSL error envelope, although they are taken from 0.47–0.94 m above the Pleistocene deposits (Fig. 6). However, it cannot be excluded that the samples of BLB2 are upper-limiting data as no botanical analysis is available. The only thing that can be stated here is that the cores are from the mainland part of the area.

While the compaction of basal peat ranges from 43 to 98% – with most samples lying between 50 and 70% – the compaction of the material (peat and sediments) underlying the intercalated peat samples ranges from 5 to 55% – with most samples lying between 35 and 55% – independent of the existence and thickness of a basal peat underneath. One explanation for this difference is that in general the intercalated peat beds are much thinner than the basal peat beds in the study area.

Especially for the basal peat samples, the compaction varies strongly in the presented dataset. For core GE176 the lower and upper extreme value of compaction is documented: 43% in the upper part of the peat layer and 98% in the lower part. The given core description as well as the geographical position of the cross section (Fig. 4) cannot explain the extreme range of compaction rates of the lower part of the basal peats. This attests to the often incalculable effect of compaction. Nevertheless, for the remaining dataset of 10 samples a decompaction rate from 1.76 to 2.89 with an average of 2.29 was calculated, which provides at least an estimate for a correction of compaction of basal peats for the study area.

The average decompaction rate of the material underneath the intercalated peat samples is less than that of the basal peats and is calculated at 1.67, although the thickness to the Pleistocene is generally higher than that of the basal peat samples. Furthermore, the thickness of the basal peat in the cores from which intercalated peat samples are taken does not seem to directly influence the amount of compaction. The variation of the decompaction factor of intercalated peat samples is independent of both the general thickness of the underlying material and the thickness of basal peat in the geological record. This supports the assumption that the main compaction process of the basal peat ended before the intercalated peat bed developed.

This agrees in principle with the findings of Smith et al. (2003) and Lloyd et al. (2013). They come to the conclusion that the compaction of the underlying peat was completed before the deposition of another regressive layer, such as an intercalated peat bed. The prerequisite for this assumption is that the thickness of the clastic overburden exceeds 2.5 m (Smith et al., 2003; Lloyd et al., 2013). The overburden observed in our cores in many cases is significantly less than 2.50 m, with values of for example 0.55 m and 1.40 m. What cannot completely be excluded here is erosion of formerly deposited material, although this is not indicated by the core descriptions.

As the dataset for the RSL curve is not complete and data from ~6000 cal BP and 3000 cal BP had to be connected by a straight line instead of a possibly more curved shape, we consider our decompaction estimates as first-order approximations which likely represent minimum values in most cases. We assume that the calculated decompaction factors are underestimated for most cases and just give a minimum value. Nevertheless, the decompaction necessary for basal peats is higher than that for samples taken from intercalated peats.

Sea-level-independent asynchronous landscape development along the coast

When comparing Holocene sedimentary records of the coastal areas between the Ems and Elbe estuaries, a different number of intercalated peat beds is noted: only one peat bed in the Stade–Buxtehude area adjacent to the Elbe estuary and up to seven intercalated peat beds in the Weser estuary (Streif, 2004). Moreover, these intercalated peat layers show inconsistent chronologies. Following the cross sections published by Streif (2004), only the uppermost peat bed has a consistent age of ~2000 BP (calendar years, not calibrated) along the coast, although the calibrated dataset presented here for Langeoog suggests the growth of the uppermost peat for ~3000 cal BP. Raised bog on top of intercalated fen peat is documented for the Jade Bay and the Ems estuary only.

We assume that the development of peat beds is driven by local sediment supply probably varying in the different tidal basins. Another reason for asynchronous development that needs to be mentioned here could be the flood basin effect (Van de Plassche, 1982; Kiden et al., 2008; Vis et al., 2015; Hijma & Cohen, 2019), which is a drop of high-water level and tidal range

https://doi.org/10.1017/njg.2021.11 Published online by Cambridge University Press

Table 3. Reconstructed factors of decompaction for basal peat samples. The average value is 2.29, excluding the three high values from core GE176 (HV4728, HV4729, HV4263; see Fig. 4). HV4263 is clearly an outlier (see Fig. 6)

Basal peat, sample ID	Depth midpoint sample to consolidated substrate (m)	Depth RSL centre line to consolidated substrate (m)	Compaction rate (%)	Decompaction factor
HV3394	1.36	2.40	43	1.76
HV4264	1.73	3.13	55	1.81
HV4261	2.06	5.26	61	2.55
HV4728	0.73	4.93	85	6.75
HV4729	0.53	4.33	88	8.17
HV4263	0.06	3.00	98	50.00
HV4267	2.03	5.13	60	2.53
HV4268	1.68	3.58	53	2.13
HV4266	1.23	3.00	59	2.44
HV4184	0.48	1.10	56	2.29
HV4187	3.46	8.16	58	2.36
HV4188	1.48	3.18	53	2.15
HV4732	1.22	3.52	65	2.89

Table 4. Reconstructed factors of decompaction for intercalated peat samples; the average value is 1.67

Intercalated peat, sample ID	Depth midpoint sample to consolidated surface (m)	Depth RSL centre line to consolidated substrate (m)	Compaction (%)	Decompaction factor	Thickness basal peat (m)	Clastic overburden on basal peat
HV3387	3.91	6.15	36	1.57	0.27	2.86
HV3388	3.66	5.61	35	1.53	0.27	2.80
HV3389	2.51	3.00	16	1.20	0.27	2.00
HV3390	2.33	2.45	5	1.05	0.27	2.00
HV3393	2.69	4.19	36	1.56	0.18	2.33
HV4270	3.60	7.80	46	2.17	1.30	1.40
HV4271	3.18	7.00	54	2.20	1.30	1.40
HV4730	1.00	1.90	47	1.90	0.38	0.57
HV4731	2.13	4.78	55	2.24	1.45	0.55
HV4183	1.53	2.70	44	1.76	0.58	0.78
HV4181	2.90	4.50	36	1.55	0.97	1.83
HV4186	7.81	10.46	25	1.34	3.50	4.40

when a tidal basin is closed off from the open sea. Behind this closing shore the influence of the tides decreases and peat starts to grow, indeed typically over large areas. Thus, across-basin occurring peat does not necessarily indicate falling sea level but locally falling high-water level in an individual tidal basin. The Flemish and Zeeland coasts have undergone several switches from closed to open basins during the Holocene (Vos & Van Heeringen, 1997; Baeteman, 1999). Also, from Flanders, Zeeland and Holland it is known that a very slowly rising sea level supports a closing coast due to onshore sediment transport (e.g. Beets & van der Spek, 2000). For the East Frisian coast, the barrier island chain is assumed to have existed since ~7 ka (Flemming & Davis, 1994), but details of its mid–late Holocene development are yet to be investigated. Anyway, in contrast to the Netherlands coast, for the East Frisian Peninsula no closing coast has been documented so far. According to historical maps (e.g. Le Coq, 1805; Homeier, 1964), the East Frisian island chain modified its shape over time, in general with islands becoming longer and thereby narrowing tidal inlets in between. However, these maps apply for the time when dikes had been built and made the coastline of the mainland static.

Notwithstanding the lack of details, for the mid–late Holocene it is documented that the mainland-shoreline prograded seawards and that mires have developed over wide areas since then (Streif, 2004; Karle et al., 2021). Furthermore, changes in strength and frequency of storm surges are crucial for the progradation or retrogradation of the coastline by erosion or redistribution of sediment. Baeteman (2005) and Karle et al. (2021) show drainage

https://doi.org/10.1017/njg.2021.11 Published online by Cambridge University Press

and compaction of marshes and peatlands initiated by the incision of channels and subsequent inundation. This results in an apparent acceleration of sea-level rise but is in fact a local relative water-level rise due to compaction effects (cf. Long et al., 2006).

For the Langeoog tidal basin it is assumed that sediment supply is the most relevant trigger for coastal progradation and peat development because tidal channels and creeks are important sediment suppliers and drainage networks for changing the depositional environment as shown by Baeteman (2013). Therefore, intercalated peats mostly reflect local sedimentary processes or perhaps local changes of water level in case of changes in tide levels, but do not generally represent changes of RSL trends. For the study area, intercalated peat beds are documented from ~5600 cal BP to ~2700 cal BP. What can be assessed here is a short phase of transgression from ~4000 cal BP to ~3800 cal BP but without any hints of sea-level acceleration or single events documented in the RSL curve and sedimentological record.

To determine whether this is just a local phenomenon for the back-barrier of Langeoog or whether it has a regional meaning for e.g. the entire East Frisian coast, other back-barrier areas will have to be analysed in the same detail (Bungenstock & Weerts, 2012). Furthermore, high-precision RSL indicators such as derived from the transgressional contact of thin basal peat beds or from a Foraminifera transfer function (Scheder et al., 2019) are needed to better quantify changes in RSL if existent.

Comparison with other regional RSL curves and assumptions on glacial isostatic adjustment (GIA)

RSL curves standardised following the HOLSEA sea-level protocol (Khan et al., 2019) are best for a direct comparison, so that artificial differences due to different approaches can be prevented. We therefore plot the MSL curve for the western Netherlands by Hijma & Cohen (2019), who work with their own data and integrate the data by van de Plassche et al. (2010). Hijma & Cohen (2019) used a combination of base-of-basal peat and top-of-basal peat data, which are non-erosively overlain by tidal deposits, with most data only 5 cm above the unconsolidated substrate (Fig. 7).

The RSL curve for Langeoog lies below the curve for the western Netherlands, nevertheless with overlapping error envelopes, while before 6000 cal BP it seems to diverge (Fig. 7), indicating that the main GIA effect is apparent before ~6000 cal BP. The offset of up to 0.80 m between 6000 and 3000 cal BP is probably mainly due to the straight course of the Langeoog curve during this timespan. More data would probably allow to scetch its course more curved and the two curves would be even closer. The calculated decompaction factors for this study had to be adjusted (accelerated). Plotting RSL curves from other coastal areas along the southern North Sea coast without correcting the data for their respective indicative meaning as provided by the HOLSEA sea-level protocol (Hijma et al., 2015; Khan et al., 2019) carries the risk of depicting the offset effect of tide data, e.g. mean high-water level, rather than the effect of GIA. The published GIA model predictions for the southern North Sea (Vink et al., 2007) are based on previously published sea-level data, not applying the later-developed standardisation provided by Khan et al. (2019). Comparing the predicted RSL curve for Wangerooge, which is ~20 km east of Langeoog, and the predicted RSL curve for the western Netherlands shows an offset of 3 m at 6000 cal BP and 1.5 m at 3000 cal BP. This is much higher than that between the RSL curve of Langeoog and the RSL curve for the western Netherlands by Hijma & Cohen (2019) with an offset in decimetre range and overlapping error envelopes.

Conclusions

The revised RSL curve for Langeoog, complemented with additional data, is significantly different from that previously published by Bungenstock & Schäfer (2009), as phases of still-stand, deceleration or strong acceleration of RSL since 6000 cal BP cannot be proven by the evaluated dataset presented here.

The subordinate progradational and retrogradational signals in the Langeoog area are supposed to mirror local effects, which are expected to vary along the German coastline as documented by Streif (2004) and Karle et al., (2021). Therefore, intercalated peat data as indicators for changes of RSL in the sense of a slowdown of sea-level rise or even a still-stand are questionable. Nevertheless, they provide important information for local coastal progradation, which is suspected to be asynchronous along the German North Sea coast. For the study area, a short phase of transgression from 4000~ cal BP to ~3800 cal BP can be assessed, but without any hints on sea-level acceleration or single events. The evaluation of sea-level index points from adjacent tidal basins will provide more information for a reliable review of the stratigraphic meaning of the intercalated peat beds along the East Frisian coast.

Overall, compaction is, as expected, a difficult factor to calculate. However, our data show that compaction of basal peats is higher than that of the sediments underlying the samples from intercalated peat beds. The necessary factors of decompaction calculated here, at 2.29 for basal peats and 1.67 for samples from intercalated peats, are probably underestimated, as they were calculated for the centre line of the presented RSL curve, which is unnaturally straight due to the few data points.

The comparison with the RSL curve for the western Netherlands shows that the Langeoog curve lies below the western Netherlands curve. In the part older than 6000 cal BP, the Langeoog RSL curve diverges from the western Netherlands curve, whereas since ~6000 cal BP the Langeoog curve is close to the RSL curve for the western Netherlands, with the Langeoog curve lying up to 0.80 m below. This difference is probably mainly due to the lack of data of the Langeoog curve and its resulting straight shape in contrast to the curved shape of the western Netherlands curve. Most probably, this difference would diminish with a better dataset for Langeoog. However, in any case this means a smaller impact of GIA for the time since 6000 cal BP than modelled so far.

The dataset presented here was not originally taken for the purpose of sea-level research and no material is left to do more detailed analysis. Overall, the Langeoog dataset is not of the quality of those used in other sea-level papers (Meijles et al., 2018; Hijma & Cohen, 2019) in terms of suitability and precision with ideally transgressive contacts on thin basal peat beds. Nevertheless, the dataset contributes a step forward towards sea-level research accordant with the new sea-level protocol (Khan et al., 2019), providing comparability and a base for further work along the German North Sea coast. In a next step, SLIPs for further tidal basins along the southern North Sea should be analysed and evaluated.

Supplementary material. Supplementary material is available online at https://doi.org/10.1017/njg.2021.11.

Acknowledgements. This contribution was greatly improved by the extremely constructive reviews of an anonymous reviewer, Patrick Kiden and Robin Edwards. A warm thanks goes to Barbara Mauz for discussion and improving the English wording. We thank the State Office for Mining and Geology of Lower Saxony (LBEG) for providing basic digital data for the Langeoog study (Scha 279/18-1). We thank Jobst Barckhausen for detailed geological

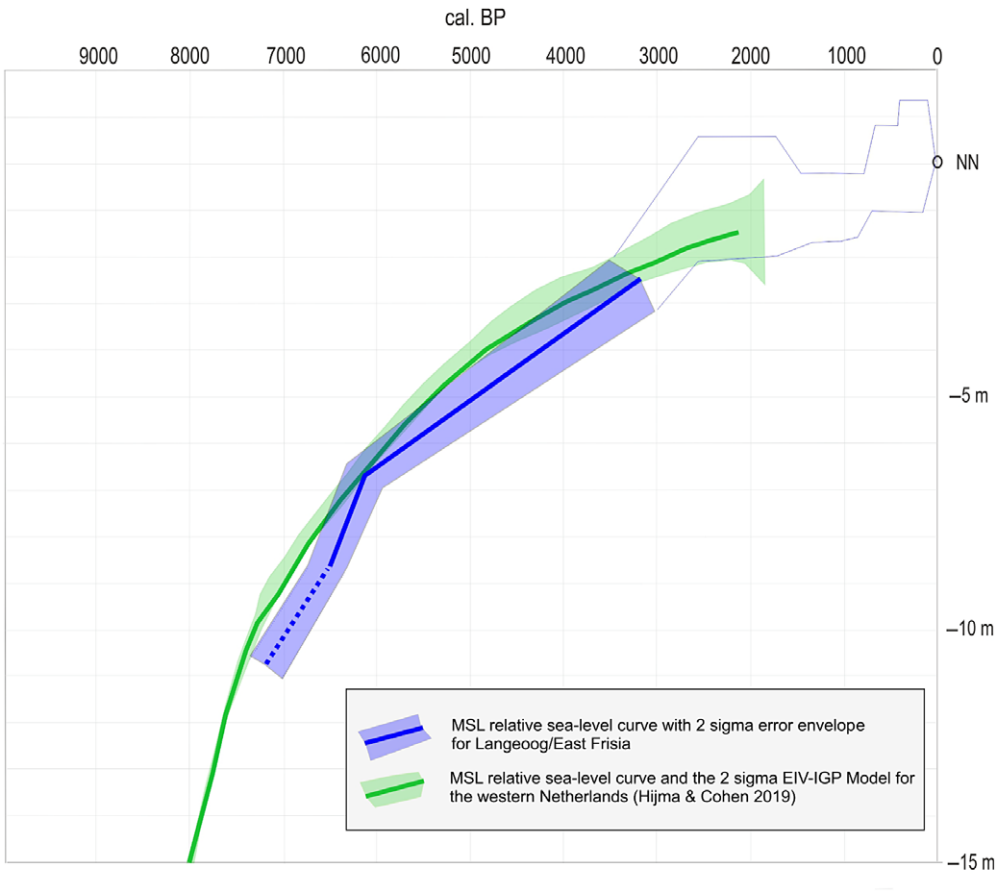

Fig. 7. The decompacted Langeoog RSL curve (see Fig. 6) and the RSL curve for the Western Netherlands by Hijma & Cohen (2019). For locations see Figure 1.

background information about the Langeoog area. Our gratitude goes to all the students and colleagues who participated in the fieldwork. This publication is dedicated in memoriam to Henk Weerts, who encouraged the main author to continue with sea-level studies.

This paper is a contribution to the IGCP project 639 'Sea level change from minutes to millennia.'

References

Baeteman, C., 1999. The Holocene depositional history of the IJzer palaeovalley (western Belgian coastal plain) with reference to the factors controlling the formation of intercalated peat beds. Geologica Belgica **2**: 39–72.

Baeteman, C., 2005. How subsoil morphology and erodibility influence the origin and pattern of late Holocene tidal channels: case studies from the Belgium coastal lowlands. Quaternary Science Reviews **24**: 2146–2162.

Baeteman, C., 2013. History of research and state of the art of the Holocene depositional history of the Belgian coastal plain. *In*: Thoen, E., Borger, G.J., de Kraker, A.M.J., Soens, T., Tys, D., Vervaet, L. & Weerts, H.J.T. (eds): Landscape or seascape? The history of the coastal environment in the North Sea area reconsidered. Brepols Publishers (Turnhout): 11–29.

Baeteman, C., Waller, M. & Kiden, P., 2011. Reconstructing middle to late Holocene sea-level change: a methodological review with particular reference to 'A new Holocene sea-level curve for the southern North Sea' presented by K.-E. Behre. Boreas **40**: 557–572.

Baeteman, C., Waller, M. & Kiden, P., 2012. Reconstructing middle to late Holocene sea-level change: a methodological review with particular reference to 'A new Holocene sea-level curve for the southern North Sea' presented by K.-E. Behre: Reply to comments. Boreas **41**: 315–318.

Barckhausen, J., 1969. Entstehung und Entwicklung der Insel Langeoog – Beispiele zur Quartärgeologie und Paläogeographie eines ostfriesischen Küstenabschnittes. Oldenburger Jahrbuch. **68**: 239–281.

Barlow, N.L.M., Shennan, I., Long, A.J., Gehrels, W.R., Saher, M.H., Woodroffe, S.A. & Hillier, C., 2013. Salt marshes as late Holocene tide gauges. Global and Planetary Change **106**: 90–110.

Beets, D.J. & van der Spek, A.J.F., 2000. The Holocene evolution of the barrier and back-barrier basins of Belgium and the Netherlands as a function of late Weichselian morphology, relative sea-level rise and sediment supply. Geologie en Mijnbouw / Netherlands Journal of Geosciences **79**: 3–16.

Behre, K.-E., 1999. Die Veränderung der niedersächsischen Küstenlinien in den letzten 3000 Jahren und ihre Ursachen. Probleme der Küstenforschung im südlichen Nordseegebiet **26**: 9–33.

Behre, K.-E., 2003. Eine neue Meeresspiegelkurve für die südliche Nordsee - Transgressionen und Regressionen in den letzten 10.000 Jahren. Probleme der Küstenforschung im südlichen Nordseegebiet **28**: 9–64.

Behre, K.-E., 2007. A new Holocene sea-level curve for the southern North Sea. Boreas **36**: 82–102.

Behre, K.-E., 2012a. Sea-level changes in the southern North Sea region: a response to Bungenstock and Weerts 2010. International Journal of Earth Sciences **101**: 1077–1082.

Behre, K.-E., 2012b. Reconstructing middle to late Holocene sea-level change: a methodological review with particular reference to 'A new Holocene sea-level curve for the southern North Sea' presented by K.-E. Behre: Comments. Boreas **41**: 108–114.

Behre, K.-E., 2012c: Die Geschichte der Landschaft um den Jadebusen, Friesland – Wilhelmshaven – Wesermarsch. Brune Mettcker Druck- und Verlagsgesellschaft (Wilhelmshaven): 280 pp.

Bennema, J., Geuze, E.C.W.A., Smits, H. & Wiggers, A.J., 1954. Soil compaction in relation to Quaternary movements of sea-level and subsidence of the land, especially in the Netherlands. Geologie en Mijnbouw **16**: 173–178.

Berendsen H.J.A., Makaske B., van de Plassche, O., van Ree, M.H.M., Das, S., van Dongen, M., Ploumen, S. & Schoenmakers, W., 2007. New groundwater-level rise data from the Rhine-Meuse Delta: implications for the

reconstruction of Holocene relative mean sea-level rise and differential land-level movements. Netherlands Journal of Geosciences **86**: 333–354.

Bos, I.J., Busschers, F.S. & Hoek, W.Z., 2012. Organic-facies determination: a key for understanding facies distribution in the basal peat layer of the Holocene Rhine-Meuse delta, The Netherlands. Sedimentology, **59** (2): 676–703.

Brain, M., 2015. Compaction. *In*: Shennan, I., Long, A.J. & Horton B.P. (eds): Handbook of sea-level research. John Wiley & Sons (Hoboken): 452–469.

BSH (Bundesamt für Seeschifffahrt und Hydrographie), 2020. Gezeitenkalender. 2020: Hoch- und Niedrigwasserzeiten für die Deutsch Bucht und deren Flussgebiete. Bundesamt für Seeschifffahrt und Hydrographie (Hamburg, Rostock): 135 pp.

Bungenstock, F., 2005. Das Küstenholozän der südlichen Nordsee – Archiv der Meeresspiegelbewegungen. *In*: Fansa, M. (ed.): Kulturlandschaft Marsch, Natur-Geschichte-Gegenwart. Landesmuseum für Natur und Mensch (Oldenburg): 37–51.

Bungenstock, F., 2006. Der holozäne Meeresspiegelanstieg südlich der ostfriesischen Insel Langeoog, südliche Nordsee: hochfrequente Meeresspiegelbewegungen während der letzten 6000 Jahre. Dissertation, Rheinische Friedrich-Wilhelms-Universität (Bonn): 130 pp.. https://nbn-resolving.org/urn:nbn:de:hbz:5N-06810

Bungenstock, F. & Schäfer, A., 2009. The Holocene relative sea-level curve for the tidal basin of the barrier island Langeoog, German Bight, Southern North Sea. Global and Planetary Change **66**: 34–51.

Bungenstock, F. & Weerts, H.J.T., 2010. The high-resolution Holocene sea-level curve for Northwest Germany: global signals, local effects or data-artefacts? International Journal of Earth Sciences **99**(8): 1687–1706.

Bungenstock, F. & Weerts, H.J.T., 2012. Holocene relative sea-level curves for the German North Sea coast. International Journal of Earth Sciences **101**: 1083–1090.

Busschers, F.S., Kasse, C., van Balen R.T., Vandenberghe, J., Cohen, K.M., Weerts, H.J.T., Wallinga, J., Johns, C., Cleveringa, P. & Bunnik, F.P.M., 2007. Late Pleistocene evolution of the Rhine-Meuse system in the southern North Sea basin: imprints of climate change, sea-level oscillation and glacio-isostacy. Quarternary Science Reviews **26**: 3216–3248.

Clerkx, A.P.P.M., Van Dort, K.W. & Hommel, P.W.F.M., 1994. Broekbossen van Nederland. IBN-rapport; 096. IBN-DLO [etc.]. https://edepot.wur.nl/390232.

Den Held, A.J., Schmitz, M. & Van Wirdum, G., 1992. Types of terrestrializing fen vegetation in the Netherlands. In Fens and bogs in the Netherlands: 237–321.

Denys, L. & Baeteman, C., 1995. Holocene evolution of relative sea level and local mean high water spring tides in Belgium - a first assessment. Marine Geology **124**: 1–19.

Edwards, R.J., 2006. Mid- to late-Holocene relative sea-level change in southwest Britain and the influence of sediment compaction. Holocene **16**: 575–587.

Engelhart, S.E. & Horton, B.P., 2012. Holocene sea level database for the Atlantic coast of the United States. Quaternary Science Reviews **54**: 12–25.

Enters, D., Haynert, K., Wehrmann, A., Freund, H. & Schlütz, F., 2021. A new ΔR value for the southern North Sea and its application in coastal research. Netherlands Journal of Geosciences **100**, e1; doi: https://doi.org/10.1017/njg.2020.19.

Ervynck, A., Baeteman, C., Demiddele, H., Hollevoet, Y., Pieters, M., Schelvis, J., Tys, D., Van Strydonck, M. & Verhaeghe, F., 1999. Human occupation because of a regression, or the cause of a transgression? A critical review of the interactions between geological events and human occupation in the Belgian coastal plain during the first millennium AD. Probleme der Küstenforschung im südlichen Nordseegebiet **26**: 97–121.

Fjeldskaar W., 1994. The amplitude and decay of the glacial forebulge in Fennoscandia. Norsk Geologisk Tidsskrift **74**: 2–8.

Flemming, B.W. & Davis, R.A., 1994. Holocene evolution, morphodynamics and sedimentology of the Spiekeroog barrier island system (Southern North Sea). Senckenbergiana maritime **24**: 117–155.

Flemming, B.W. & Nyandwi, N., 1994. Land reclamation as a cause of fine-grained sediment depletion in back-barrier tidal flats (southern North Sea). Netherlands Journal of Aquatic Ecology **28**: 299–307.

Gehrels, W.G. & Shennan, I., 2015. Sea level in time and space: revolutions and inconvenient truths. Journal of Quaternary Science **30**(2): 131–143.

Gehrels, W.R., Callard, S.L., Moss, P.T., Marshall, W.A., Blaauw, M., Hunter, J., Milton, J.S. & Garnett, M.H., 2012. Nineteenth and twentieth century sea-level changes in Tasmania and New Zealand. Earth and Planetary Science Letters **315–316**: 94–102.

Griffel, G., Asprion, U. & Elbracht, J., 2013. Die neue Holozänbasis der niedersächsischen Nordseeküste. Geopotenzial Deutsche Nordsee ww.gpdn.de: https://www.gpdn.de/iwilma.ashx?request=getMedia&ts=635207239475470000&mediaId=1408.

Haarnagel, W., 1950. Das Alluvium an der deutschen Nordseeküste. Probleme der deutschen Küstenforschung im südlichen Nordseegebiet 4: 146 pp.

Hepp, D.A., Romero, O.E., Mörz, T., De Pol-Holz, R. & Hebbeln, D., 2019. How a river submerges into the sea: a geological record of changing a fluvial to a marine paleoenvironment during early Holocene sea level rise. Journal of Quaternary Science **34**(7): 581–592.

Hertweck, G., 1993. Zeitliche Variabilität und räumliche Inhomogenität in den Substrateigenschaften und der Zoobenthosbesiedlung im Umfeld von Miesmuschelbänken. A. Biofazies und Aktuopaläontologie. Berichte Senckenberg am Meer **93**(1): 49–63.

Hijma, M. P. & Cohen, K. M., 2019. Holocene sea-level database for the Rhine-Meuse Delta, The Netherlands: implications for the pre-8.2 ka sea-level jump. Quaternary Science Reviews, **214**: 68–86.

Hijma, M.P., Engelhart, S.E., Törnqvist, T.E., Horton, B.P., Hu, P. & Hill, D.F., 2015. A protocol for a geological sea-level database. *In*: Shennan, I., Long, A.J. & Horton B.P. (eds): Handbook of sea-level research. John Wiley & Sons (Hoboken:): 536–554.

Homeier, H., 1964: Niedersächsische Küste. Historische Karte 1:50.000, Nr. 5 Osterems mit Memmert bis Mitte Norderney. 4 Karten mit Beiheft. Forschungsstelle Norderney der Niedersächsischen Wasserwirtschaftsverwaltung (Norderney).

Horton, B.P. & Shennan, I., 2009. Compaction of Holocene strata and the implications for relative sea-level change on the east coast of England, Geology **37**: 1083–1086.

Jelgersma, S., 1961. Holocene sea-level changes in the Netherlands. Mededelingen Geologische Stichting C-IV. **7**: 1–100.

Jelgersma, S., 1979. Sea-level changes in the North Sea Basin. *In*: Ole, E., Schüttenhelm, R.T.E. & Wiggers, A.J. (eds): The Quaternary history of the North Sea. Uppsala University (Uppsala): 233–248.

Karle, M., Bungenstock, F. & Wehrmann, A., 2021. Holocene coastal landscape development – sedimentary response to a rising sea level at the Central Wadden Sea coast. Netherlands Journal of Geosciences **100**, e12; doi: https://doi.org/10.1017/njg.2021.10.

Kaye, C.A. & Barghoorn, E.S., 1964. Late Quaternary sea-level change and crustal rise at Boston, Massachusetts, with notes on the autocompaction of peat. GSA Bulletin **75**(2): 63–80.

Kemp, A.C., Horton, B.P., Vane, C.H., Bernhardt, C.E., Corbett, D.R., Engelhart, S.E., Anisfeld, S.C., Parnell, A.C. & Cahill, N., 2013. Sea-level change during the last 2500 years in New Jersey, USA. Quaternary Science Reviews **81**: 90–104.

Khan, N.S., Horton, B.P., Engelhart, S., Rovere, A., Vacchi, M., Ashe, E.L., Törnqvist, T.E., Dutton, A., Hijma, M.P., Shennan, I., and the HOLSEA working group, 2019. Inception of a global atlas of sea levels since the Last Glacial Maximum. Quaternary Science Reviews **220**: 359–371.

Kiden, P., 1995. Holocene relative sea-level change and crustal movement in the southwestern Netherlands. Marine Geology **124**: 21–41.

Kiden, P., Denys, L. & Johnston, P., 2002. Late Quaternary sea-level change and isostatic and tectonic land movements along the Belgian-Dutch North Sea coast: geological data and model results. Journal of Quaternary Science **17** (5–6): 535–546.

Kiden, P., Makaske, B. & van de Plassche, O., 2008. Waarom verschillen de zeespiegel – reconstructies voor Nederland? Grondbor & Hamer **3/4**: 54–61.

Klausnitzer, B. (ed.), 2019: Stresemann - Exkursionsfauna von Deutschland - Bd. 1 Wirbellose (ohne Insekten). 9. Aufl. Springer Verlag (Berlin): 735 pp.

Lambeck K., 1995. Late Devensian and Holocene shorelines of the British Isles and North Sea from models of glacio-hydroisostatic rebound. Journal of the Geological Society of London **152**: 437–448.

https://doi.org/10.1017/njg.2021.11 Published online by Cambridge University Press

Lambeck, K, Smither, C. & Johnston, P., 1998. Sea-level change, glacial rebound and mantle viscosity for northern Europe. Geophysical Journal International **134**: 102–144.

Lange, W. & Menke, B., 1967. Beiträge zur frühglazialen erd- und vegetationsgeschichtlichen Entwicklung im Eidergebiet, insbesondere zur Flussgeschichte und zur Genese des sogenannten Basistorfes. Meyniana 17: 29–44.

LeCoq, K.L.J.E., 1805. Topographische Karte in 22 Blättern den größten Theil von Westphalen enthaltend, so wie auch das Herzogthum Westphalen und einen Theil der hannövrischen, braunschweigischen u. heßischen Länder; nach astronomischen und trigonometrischen Ortsbestimmungen. Berlin.

Lloyd, J.M., Zong, Y., Fish, P. & Innes, J.B., 2013. Holocene and Lateglacial relative sea-level change in north-west England: implications for glacial isostatic adjustment models. Journal of Quaternary Science, **28**(1): 59–70.

Long, A.J., Waller, M.P. & Stupples, P., 2006. Driving mechanisms of coastal change: peat compaction and the destruction of late Holocene coastal wetlands. Marine Geology **225**: 63–84.

Louwe-Kooijmans, L.P. & Knip, A.S., 1974. The Rhine/Meuse Delta; four studies on its prehistoric occupation and Holocene geology. Analecta Praehistoria Leidensia VII **7**: 1–78.

Louwe Kooijmans, L.P., 1976. Prähistorische Besiedlung im Rhein-Maas-Deltagebiet und die Bestimmung ehemaliger Wasserhöhen. Probleme der Küstenforschung im Südlichen Nordseegebiet **11**: 119–143.

Makaske, B., Van Smeerdijk, D.G., Peeters, H., Mulder, J.R. & Spek, T., 2003. Relative water-level rise in the Flevo lagoon (The Netherlands), 5300–2300 cal. yr BC: an evaluation of new and existing basal peat time–depth data. Netherlands Journal of Geosciences **82**: 115–131.

Mai, S. & Bartholomä, A., 2000. The missing mud flats of the Wadden Sea: a reconstruction of sediments and accommodation space lost in the wake of land reclamation. Proceedings in Marine Science **2**: 257–272.

Mauz, B. & Bungenstock, F., 2007. How to reconstruct trends of late Holocene relative sea level: a new approach using tidal flat clastic sediments and optical dating. Marine Geology **237**: 225–237.

Mauz, B., Bode, T., Mainz, E., Blanchard, H., Hilger, W., Dikau, R. & Zöller, L., 2002. The luminescence dating laboratory at the University of Bonn: equipment and procedures. Ancient TL **20**: 53–61.

Mauz, B., Baeteman, C., Bungenstock, F. & Plater, A.J., 2010. Optical dating of tidal sediments: potentials and limits inferred from the North Sea coast. Quaternary Geochronology **5**: 1–12.

Meier, D., Kühn, H.J. & Borger, G.J., 2013. Der Küstenatlas, Das schleswig-holsteinische Wattenmeer in Vergangenheit und Gegenwart. Boyens (Heide): 1991 pp.

Meijles, E.W., Kiden, P., Streurman, H.-J., Van der Plicht, J., Vos, P.C., Gehrels, W.R. & Kopp, R.E., 2018. Holocene relative mean sea-level changes in the Wadden Sea area, northern Netherlands. Journal of Quaternary Science **33**: 905–923.

Newell, R., 1962. Behavioural aspects of the ecology of Peringia (= Hydrobia) ulvae (Pennant) (Gasteropoda, Prosobranchia). Proceedings of the Zoological Society of London **138**(1): 49–75.

NIBIS® Map Server, 2014a. Boreholes and profiles. Landesamt für Bergbau, Energie und Geologie (LBEG) (Hannover).

NIBIS® Map Server, 2014b. Relief of the Holocene basis. Landesamt für Bergbau, Energie und Geologie (LBEG) (Hannover).

Nilsson, T., 1949. Versuch einer Anknüpfung der postglazialen Entwicklung des nordwestdeutschen und niederländischen Flachlandes an die Pollenfloristische Zonengliederung Südskandinviens. Meddelanden från Lunds geologisk-mineralogiska Institution 112: 79 pp.

Paul, M.A. & Barras, B.F., 1998. A geotechnical correction for postdepositional sediment compression: examples from the Forth Valley, Scotland. Journal of Quaternary Science **13**: 171–176.

Peltier, W.R., 2004. Global glacial isostasy and the surface of the ice-age Earth: the ICE-5G (VM2) model and GRACE. Annual Review of Earth and Planetary Sciences **32**: 111–149.

Preuß, H., Vinken, R. & Voss, H.-H., 1991. Symbolschlüssel Geologie, 3rd edn. Niedersächsisches Landesamt für Bodenforschung und Bundesanstalt für Geowissenschaften und Rohstoffe (Hannover): 328 pp.

Reimer, P., Austin, W.E.N., Bard, E., Bayliss, A., Blackwell, P.G., Bronk Ramsey, C., Butzin, M., Cheng, H., Edwards, R.L., Friedrich, M., Grootes, P.M., Guilderson, T.P., Hajdas, I., Heaton, T.J., Hogg, A.G., Hughen, K.A., Kromer, B., Manning, S.W., Muscheler, R., Palmer, J.G., Pearson, C., van der Plicht, J., Reimer, R.W., Richards, D.A., Scott, E.M., Southon, J.R., Turney, C.S.M., Wacker, L., Adolphi, F., Büntgen, U., Capano, M., Fahrni, S., Fogtmann-Schulz, A., Friedrich, R., Köhler, P., Kudsk, S., Miyake, F., Olsen, J., Reinig, F., Sakamoto, M., Sookdeo, A. & Talamo, S., 2020. The IntCal20 Northern Hemisphere radiocarbon age calibration curve (0-55 cal kBP). Radiocarbon 62. doi: 10.1017/RDC.2020.41.

Reineck, H.-E. & Siefert, W., 1980. Faktoren der Schlickbildung im Sahlenburger und Neuwerker Watt. Die Küste **35**: 26–51.

Roeleveld, W., 1974. The Holocene evolution of the Groningen Marine-Clay District. Berichten van de Rijksdienst voor het Oudheidkundig Bodemonderzoek 24, Supplement ('s-Gravenhage).

Roeleveld, W. & Gotjé, W., 1993. Holocene waterspiegelontwikkeling in de Noordoostpolder in relatie tot zeespiegelbeweging en kustontwikkeling. *In*: De Holocene laagveenontwikkeling in de randzone van de Nederlandse kustvlakte (Noordoostpolder). PhD Thesis. Vrije Universiteit Amsterdam (Amsterdam): 76–86.

Roep, T.B. & Beets, D.J., 1988. Sea level rise and paleotidal levels from sedimentary structures in the coastal barriers in the western Netherlands since 5600 BP. Geologie en Mijnbouw **67**: 53–60.

Scheder, J., Frenzel, P., Bungenstock, F., Engel, M., Brueckner, H. & Pint, A., 2019. Vertical and lateral distribution of Foraminifera and Ostracoda in the East Frisian Wadden Sea: developing a transfer function for relative sea-level change. Geologica Belgica **22**(3–4): 99–110.

Schmid, P., 1993. Siedlungsarchäologische Ergebnisse zur Vor- und Frühgeschichte. *In:* Elzholz, E. (ed.): Nordenham. Geschichte einer Stadt. Isensee (Oldenburg): 13–50.

Schückel, U., Beck, M. & Kröncke, I., 2013. Spatial variability in structural and functional aspects of macrofauna communities and their environmental parameters in the Jade Bay (Wadden Sea Lower Saxony, southern North Sea). Helgoland Marine Research **67**: 121–136.

Schütte, H., 1939. Sinkendes Land an der Nordsee. Schriften des Deutschen Naturkundevereins / NF 9: 144 pp.

Shennan, I., Lambeck, K., Flather, R., Horton, B., McArthur, J., Innes, J., Lloyd, J., Rutherford, M. & Wingfield, R., 2000. Modelling western North Sea palaeogeographies and tidal ranges during the Holocene. *In:* Shennan, I. & Andrews, J. (eds.): Holocene land–ocean interaction and environmental change around the North Sea. Geological Society of London, Special Publication 166: 299–319.

Shennan, I., Hamilton, S., Hillier, C. & Woodroffe, S., 2005. A 16,000-year record of near-field relative sea-level changes, northwest Scotland, United Kingdom. Quaternary International **133–134**: 95–106.

Smith, D.E, Wells, J.M, Mighall, T.M., Cullingford, A.A., Holloway, L.K., Dawson, S. & Brooks, S.L., 2003. Holocene sea levels and coastal changes in the lower Cree valley and estuary, SW Scotland, U.K. Earth Sciences **93**: 301–331.

Steffen, H., 2006. Determination of a consistent viscosity distribution in the Earth's mantle beneath Northern and central Europe. PhD Thesis, Institut für Geologische Wissenschaften der Freie Universität Berlin (Berlin): 137.

Streif, H., 1971. Stratigraphie und Faziesentwicklung im Küstengebiet von Woltzeten in Ostfriesland. Beihefte Geologisches Jahrbuch 119: 59 pp.

Streif, H., 1990. Das ostfriesische Küstengebiet – Nordsee, Inseln, Watten und Marschen. Sammlung geologischer Führer, Band **57**: 376 pp.

Streif, H., 2004. Sedimentary record of Pleistocene and Holocene marine inundations along the North Sea coast of Lower Saxony, Germany. Quaternary International **112**: 3–28.

Van Asselen, S., 2011. The contribution of peat compaction to total basin subsidence: implications for the provision of accommodation space in organic-rich deltas. Basin Research **23**(2): 239–255.

Van de Plassche, O., 1982. Sea-level change and water-level movements in the Netherlands during the Holocene. Mededelingen Rijks Geologische Dienst 36(1): 1–93.

Van de Plassche, O. & Roep, T.B., 1989. Sea-level changes in the Netherlands during the last 6500 years: basal peat vs. coastal barrier delta. *In*: Scott, D.B., Pirazzoli, P.A. & Honig, C.A. (eds): Late Quaternary sea-level correlation and applications. Kluwer Academic Publishers (Dordrecht): 41–56.

https://doi.org/10.1017/njg.2021.11 Published online by Cambridge University Press

Van de Plassche, O., Bohncke, S.J.P., Makaske, B. & Van der Plicht, J., 2005. Water-level changes in the Flevo area, central Netherlands (5300–1500 BC): implications for relative mean sea-level rise in the Western Netherlands. Quaternary International 133–134, 77–93.

Van de Plassche, O., Makaske, B., Hoek, W.Z., Konert, M. & van der Plicht, J., 2010. Mid-Holocene water-level changes in the lower Rhine-Meuse Delta (western Netherlands): implications for the reconstruction of relative mean sea-level rise, palaeoriver-gradients and coastal evolution. Netherlands Journal of Geosciences **89**: 3–20.

Van der Molen, J. & de Swart, H.E., 2001. Holocene tidal conditions and tide-induced sand transport in the southern North Sea. Journal of Geophysical Research **106**(C5): 9339–9362.

Van der Spek, A., 1996. Holocene despositional sequences in the Dutch Wadden Sea south of the island of Ameland. Mededelingen Rijks Geologische Dienst, 57: 41–68.

Vink, A., Steffen, H., Reinhardt, L. & Kaufmann, G., 2007. Holocene relative sea-level change, isostatic subsidence and the radial viscosity structure of the mantle of northwest Europe (Belgium, the Netherlands, Germany, southern North Sea). Quaternary Science Reviews **26**: 3249–3275.

Vis, G.-J-, Cohe, K.M., Westerhoff, W.E., Ten Veen, J.H., Hijma. M.P., Van der Spek, A.J.F. & Vos, P.C., 2015. Paleogeography. *In*: Shennan, I., Long, A.J. & Horton B.P. (eds): Handbook of sea-level research. John Wiley & Sons (Hoboken): 514–535.

Vos, P.C. & van Heeringen, R.M., 1997. Holocene geology and occupation history of the Province of Zeeland. Mededelingen Nederlands Instituut voor Toegepaste Geowetenschappen TNO 59: 5–109.

Wolters, S, Zeiler, M. & Bungenstock, F., 2010. Early Holocene environmental history of sunken landscapes: pollen, plant macrofossil and geochemical analyses from the Borkum Riffgrund, southern North Sea. International Journal of Earth Sciences (Geol Rundschau) 99: 1707–1719.

Zhang, J., Tsukamoto, S., Grube, A. & Frechen, M., 2014. OSL and ^{14}C chronologies of a Holocene sedimentary record (Garding-2 core) from the German North Sea coast. Boreas **43**(4): 856–868.

https://doi.org/10.1017/njg.2021.11 Published online by Cambridge University Press